Noise Temperature and Gain Loss due to Paints and Primers: A Case Study of DSN Antennas

T. Y. Otoshi, Y. Rahmat-Samii, R. Cirillo, Jr., and J. Sosnowski

Jet Propulsion Laboratory, California Institute of Technology
4800 Oak Grove Drive, Pasadena, CA 91109
Tel: (818) 354-5699, FAX: (818) 393-4683
E-mail: tyo@jpl.nasa.gov
Department of Electrical Engineering
University of California, Los Angeles, CA 90094
Tel: (310) 206-3847, E-mail: rahmat@ee.ucla.edu

Submitted for publication to:
IEEE Antennas and Propagation Magazine

Abstract

In achieving high performance for reflector antennas, it has been noted that it is essential to carefully assess the roles of surface paints and primers. A thorough literature search has revealed that not much has been reported on this very important engineering implementation topic. It is one of the main objectives of this feature article to provide a detailed study on the effects of paints and primers on the reflector antenna performance. In particular, as a case study, this paper presents excess noise temperature and added-gain loss data at 32 GHz for various combinations of paints and primers currently being studied for use on DSN (Deep Space Network) antenna reflector surfaces. It is shown that 500FHR6 acrylic urethane-based paint has the lowest excess noise-temperature contribution. Recently, it has been recommended to use this paint for all new DSN beam-waveguide antennas being constructed and for all those 34-m and 70-m antennas whose reflector surfaces need repainting. The results, methodologies and observations presented in this article are also applicable to other reflector antenna configurations.

I. INTRODUCTION

Background on Paint Study:

Large reflector antennas are one of the key components of any communication and tracking systems. The main parameters dictating their electrical performance are the overall antenna system gain and noise temperature. These parameters are affected by many factors, such as, aperture size, aperture tapered illumination, surface tolerance, feed spillover, strut blockage and diffraction, surface conductivity resulting from protective paint, etc.

Considerable amount of work has been directed towards optimizing every aspect of these factors except the microwave properties of the paint. This is, in particular, an important issue when one deals with extremely sensitive and high performance antenna systems for deep space applications. A thorough literature search revealed that very little information has been published on the microwave properties of paints and primers used on antenna reflector surfaces. A paint study was initiated to determine how much degradation of antenna noise temperature and gain occur as functions of paint thickness on antenna reflector surfaces. In this article the paint study, noise temperature and gain loss data will be presented for various combinations of paints and primers as functions of paint thickness, incidence angle, and polarization. In particular, as a case study, this paper presents excess noise temperature and added-gain loss data at 32 GHz for various combinations of paints and primers currently being studied for use on DSN (Deep Space Network) antenna reflector surfaces. It is shown that 500FHR6 acrylic urethane-based paint has the lowest excess noise-temperature contribution and should be used for all new DSN beam-waveguide antennas being constructed and for all those 34-m and 70-m antennas whose reflector surfaces need repainting. The results, methodologies and observations presented in this article are also applicable to other high performance reflector antenna systems.

Background on DSN Antennas:

The Deep Space Network (DSN) operates with a worldwide network of three 70-m-diameter antennas, three 34-m-diameter high-efficiency antennas, and four 34-m-diameter beam-waveguide (BWG) antennas [1]. The large diameters and high aperture efficiencies of these antennas result into high gain in both receive and transmit modes. Additionally, in the receive

mode the antenna systems are designed to have very low system noise temperatures. Increasing gain and lowering system noise temperatures translate into maximizing the ground-received signal-to-noise ratio [2]. Over the years, a great deal of attention has been paid to lowering system noise temperatures through the use of low-loss front-end microwave waveguide components and cryogenically cooled low-noise amplifiers (masers and high-electron mobility transistors). A noise contributor that has not been studied with the same degree of attention in the past is the paint on the antenna main reflector surface, subreflector surface, and subreflector support legs. All DSN antennas (70-m and 34-m diameter) have main- and subreflector-reflector surfaces that are painted with layers of white thermal diffusive paint to reduce solar heating and keep the reflector surfaces close to the outdoor ambient temperature.

Figure 1 shows a view of a 34-m BWG antenna depicting the solid and perforated panel sections of the main reflector. Both the solid and perforated panels are made from 6061-T6 aluminum sheets that are painted with a layer of zinc chromate primer layer and a layer of Triangle no. 6 thermal diffusive white paint [3]. Figure 2 shows the subreflector, which is also painted with zinc chromate primer and Triangle no. 6 paint. The subreflector support legs, also shown in Fig. 2, are made from structural steel and painted with organic zinc primer and Triangle no. 710 thermal reflective white paint [4]. The first focal point of this BWG system is the normal Cassegrain focus located close to the vertex of the main reflector, while the final focal point is about 35 m and six additional mirrors distant in a subterranean room. Figure 3 shows one of the six BWG mirrors whose surfaces were painted with zinc chromate primer to keep the aluminum surfaces from oxidizing. It should be pointed out that the only BWG mirrors that have zinc chromate primer protective coatings are those for the first NASA/JPL BWG antenna that was built in 1990 at Deep Space Station 13 (DSS 13) for research and development purposes. BWG antennas that were built later for DSN operational purposes have aluminum mirror surfaces that were given an irridite surface treatment only. For predicted performance comparison purposes [5], it was of interest to know how much of the total system noise temperature on the DSS 13 BWG antenna was contributed by the paint on the main reflector and subreflector surfaces and zinc chromate primer on the six BWG mirrors. It was also of interest to accurately determine the noise temperature contributions from paints and primers on all DSN antennas.

II. THEORETICAL/NUMERCIAL APPROACHES

In conjunction with the use of experimental methods for determining the complex dielectric constant of paints, applicability of various theoretical/numerical approaches was also investigated. For completeness of reporting on this paint study, the results of these studies are summarized in the following subsections. It is commonly thought that if the complex dielectric constants of the individual paint ingredients and their volumetric ratios are known, then it should be possible to derive theoretical formulas for calculating the overall complex dielectric constant of the paint mixture. The term "volumetric ratio" is defined here as the ratio of the volume of a particular ingredient to the sum of the volumes of all the ingredients.

A. Two-Mix Ingredient Model

One of the suggested theoretical methods investigated was the two-mix formula method [6,7]. This formula has been used successfully in the past to compute complex dielectric constants of a mixture of salt in distilled water, microballoon inclusions in polymer epoxy resin [8], and artificial dielectrics.

In order to use this two-mix-ingredient formula for Triangle no. 6 paint (a patented paint), which has three main ingredients, it was necessary to use the formula two ingredients at a time. For the first step, the complex relative dielectric constants and volumetric ratios of two of the ingredients with smaller volumetric ratios were input into the quadratic equation given in [7]. The solved equation resulted in a complex relative dielectric constant of (4.87-j0.085) for the mix. The second step was to take this new equivalent single ingredient and mix it with the main ingredient, titanium dioxide (TiO_2), whose volumetric ratio was known and was assumed to have a complex relative dielectric constant value of approximately (80-j0.020) at 32 GHz [9,10]. The overall complex relative dielectric constant of the three main ingredients of Triangle no. 6 paint was calculated to be (15.2-j0.07). Other small volumes of solvents used in Triangle no. 6 were ignored because all solvents eventually evaporate. Since the actual volumetric ratios and names of some of the other ingredients used in Triangle no. 6 paint may be a trade secret, this information will not be revealed in this article. However, this information is not necessary for this article, since it is intended that only the theoretical procedure and results are presented.

This theoretically calculated complex relative dielectric constant of (15.2-j0.07) for Triangle no. 6 paint is significantly different from the measured value of (5.9-j0.15) at 32 GHz [3]. It is concluded that the theoretical two-mix-ingredient formula, valid for dry ingredient mixtures, cannot be used to accurately calculate the complex dielectric constant of paints because solvents used in the mix cause chemical changes of the combined ingredients.

B. Equivalent Circuit Model

Another suggested theoretical technique investigated was to represent individual paint ingredients as slabs of equal length and width but of different heights inside a parallel plate waveguide [11]. Then, for each individual slab, formulas for an equivalent capacitance and resistance were derived. It was assumed that the capacitance and resistance value for each slab could be expressed in terms of its complex relative dielectric constant and slab height [12], where the height is proportional to the paint ingredient's volumetric ratio. Then the individual capacitors and resistors were put in series. The final steps were to calculate the overall equivalent capacitance and equivalent resistance and convert them back to an overall complex relative dielectric constant. This technique gave a complex relative dielectric constant value of (7.02-j0.01) as compared with a measured value of (5.9-j0.15). Although this method gave a value reasonably close to the measured value for the real part of the complex relative dielectric constant, it is not known if the assumptions used in this equivalent circuit-modeling method are valid.

C. S-Parameters Measurements and Dielectric Constant Extraction

A waveguide measurement technique to determine the dielectric constant of a very thin (0.25-mm) film of paint sample is described in [13]. The real part of the complex relative dielectric constant of the paint sample in WR42 waveguide was measured to be 4.5 at 19.9 GHz. However, the measurement technique did not yield information on the loss tangent needed for determination of noise temperatures.

It appears that the only accurate way to determine both the real and imaginary parts of the complex relative dielectric constants of paints is through measurement methods such as the one

described in [3,4], which involved measurement of the S-parameters of paint test samples several wavelengths long in waveguide. For the results of the article, an automated network analyzer (HP 8510C) was used to measure the S-parameters over a wide frequency range of 23 through 35 GHz. If all four S-parameters are measured, then two data sets are obtained. The first is the (S11, S21) data set, and the second the (S22, S12) data set. The basic theory and equations for extracting complex constant from measured S-parameter data can be found in [14,15]. Due to the unknown electrical length (with multiples of 360 deg. of phase that need to be included), these equations will give a multiplicity of possible solutions for the relative dielectric constant that fits the measured S-parameter data and the given physical test-sample length. Two methods described in [3,4] were used to find and verify the unique solution for the complex dielectric constant of the test sample. After determining the complex relative constants of the paint samples, the final step is to use another computer program that calculates the S-parameters for individual paint and primer layers represented as flat dielectric sheets with the desired thicknesses and complex dielectric-constant values that were measured. Finally, the S-parameters are cascaded and the input reflection coefficient of the multilayer dielectric stack is computed for the case where the dielectric stack is terminated with the metallic reflector surface of known conductivity, such as 6061 aluminum. An alternative to using S-parameter cascading equations is to use equations that were derived specifically for studying properties of multilayer dielectric sheets on a reflector surface [16].

III. EXCESS NOISE TEMPERATURE AND ADDED-GAIN LOSS

In order to estimate the "excess noise temperature and added-gain loss" for a painted reflector antenna, a computational method was applied based on electromagnetic wave reflection from a multilayer structure. A computer program for calculating reflection and transmission coefficients of a multilayer dielectric stack [16] was provided by the University of California, Los Angeles (UCLA) Electrical Engineering Department. The inputs to the UCLA computer program are perpendicular or parallel polarization, frequency, incidence angle, ϵ_r' (see Table 1), the electrical conductivity, and thickness for each layer in the multilayer stack. For the results at 32 GHz in this article, the measured dielectric constant and electrical conductivity values shown in Table 1 were used. Figure 4 depicts the schematic of the geometrical configuration of the multilayer structure.

To employ the UCLA program for the painted reflector case, the final dielectric layer of the stack was chosen to be a thick 6061-T6 aluminum sheet, which is the material used for the reflector surfaces of DSN antennas. When a thick metallic plate is used as the last layer, the useful outputs of the UCLA program are the overall multilayer input voltage reflection coefficient (magnitude and phase) and return loss in dB. A second program was written to input the reflection coefficient values and compute noise temperatures and gain losses for perpendicular and parallel polarizations from the equations that will be given next.

In practice, what is measured is the total noise temperature of a reflector surface coated with paint and primer layers. Often the changes of noise temperature due to these paint and primer layers are so small that it is difficult to show these changes on a total noise-temperature plot. Therefore, in this article, the contribution of the paint and primer layers only will be shown. This contribution is defined as excess noise temperature, whose equation will be derived and shown below.

Once the input reflection coefficient is known for a particular paint/primer thickness, incidence angle, and polarization, the overall noise temperature of a painted reflector can be calculated from

$$T_n = \left(1 - |\Gamma_{in}|^{2N}\right) T_p \tag{1}$$

where

Γ_{in} = the input voltage reflection coefficient as seen looking at the painted reflector. It applies to a particular polarization and incidence angle.

N = the number of times that the incident wave reflects off identical reflectors in cascade before arriving at cold sky.

T_p = the physical temperature of the reflector surface, *K*.

If one is interested in the excess noise-temperature (ENT) contribution due to paint or primer or both, the following equation applies for the *N* number of reflectors case:

$$\begin{aligned} \Delta T_n &= T_{n2} - T_{n1} \\ &= \left(1 - |\Gamma_2|^{2N}\right)T_p - \left(1 - |\Gamma_1|^{2N}\right)T_p \end{aligned} \tag{2}$$

where Γ_1 and Γ_2 are the input voltage reflection coefficients as seen looking at the unpainted (bare metal) and painted reflector surfaces, respectively. There are no restrictions in Eq. (2) regarding the value of *N*. It is required only that the values of $|\Gamma_1|$ and $|\Gamma_2|$ be less than or equal to unity and greater than or equal to zero. It also is required that $|\Gamma_1| \geq |\Gamma_2|$. Note that if *N* becomes very large, $|\Gamma_{in}|^{2N}$ in Eq. (1) will go towards zero and T_n approaches being equal to T_p, as it should. In addition, when *N* becomes large, the excess noise temperature given by Eq. (2) will go towards zero.

For low-loss cases and $N \leq 10$ cases, an approximate expression for ENT can be derived as follows. Let

$$|\Gamma_1|^2 = \left(1 - x_1\right) \tag{3}$$

$$|\Gamma_2|^2 = \left(1 - x_2\right) \tag{4}$$

Then using a series expansion and dropping off higher-order terms,

$$|\Gamma_1|^{2N} = (1 - x_1)^N \sim 1 - Nx_1 \quad for \begin{cases} x_1 \leq 0.01, \\ N \leq 10 \end{cases} \tag{5}$$

$$|\Gamma_2|^{2N} = (1 - x_2)^N \sim 1 - Nx_2 \quad for \begin{cases} x_2 \leq 0.01 \\ N \leq 10 \end{cases} \tag{6}$$

Substitution of Eqs. (5) and (6) into Eq. (2) gives an approximate equation for ENT of

$$\Delta T_n \sim N(x_2 - x_1)T_p \tag{7}$$

The purpose of deriving this approximate expression is to show that for low loss or the $x_1, x_2 << 1$ and $N \leq 10$ cases, the ENT for the N mirror case is approximately equal to N times the ENT for the $N = 1$ mirror case.

Also of interest is the added-gain loss due to the paint and primer on a reflector surface. Added-gain loss is defined as the total gain loss of the lossy reflector with the paint and primer layers minus the gain loss of the reflector only. For the N number of similarly painted mirror case, the added-gain loss expressed in positive dB is

$$\begin{aligned} \Delta G_{dB} &= 10\log_{10}|\Gamma_1|^{2N} - 10\log_{10}|\Gamma_2|^{2N} \\ &= N\left(10\log_{10}|\Gamma_1|^2 - 10\log_{10}|\Gamma_2|^2\right) \end{aligned} \tag{8}$$

Note that the added-gain loss for the N mirror case is exactly equal to N times the added-gain loss for the single $N = 1$ mirror case. This equation can be used for any value of N, but it is required that the values of $|\Gamma_1|$ and $|\Gamma_2|$ be less than or equal to unity and greater than zero, and it is required that $|\Gamma_1| \geq |\Gamma_2|$.

The appropriate reflection coefficient for perpendicular or parallel polarization is used in the above equations to obtain excess noise temperatures for perpendicular and parallel polarizations. The excess noise temperature for circular polarization is obtained by taking the average of the excess noise temperatures of perpendicular and parallel polarizations [17].

IV. RESULTS AND PERFORMANCE CHARACTERIZATIONS

A. General Comments

In order to provide an easy reference for design parameters used in this article, Fig. 4 shows the schematic configuration of the various cases. The range of parameters used are indicated in Tables 1 and 2. Even though Table 1 shows only values measured in the 31–33 GHz region, complex dielectric constant values were also measured over a frequency range of 23 to 35 GHz for most of the paint samples [3,4].

The plots are shown for incidence angles from 0 to 60 deg for 32 GHz. The 60-deg limit was chosen for the following reason: Although the maximum incidence angle is about 30 deg for the main-reflector and is less for subreflector surfaces, some of the reflectors in a beam-waveguide (BWG) antenna system have incidence angles of 45 deg. One of the BWG mirrors has an incidence angle of about 60 deg near its edges. Stray signal reflections off the BWG shroud walls can have incidence angles of 60 deg or greater, and hence these plots can also be useful for BWG shroud noise-temperature contribution analyses.

Even though the results presented in this article apply to the plane-wave case, plane-wave solutions can be applied to small localized areas of curved mirrors. It was shown in [16] that, when localized individual plane wave contributions were added up, good results for the entire curved surface antenna were obtained.

For all noise temperatures and excess noise temperatures presented in this article, the operating frequency is 32 GHz, and paints, primers, and reflectors are at a physical temperature of 293.2 K (20 deg C).

B. Plots as Functions of Incidence Angles

Figures 5a and 5b show the total noise temperature and gain loss, respectively, of a 6061-T6 flat mirror for perpendicular and parallel polarizations. The noise-temperature and gain-loss values for 6061-T6 aluminum are based on an electrical conductivity of 2.3×10^7 mhos/m [18]. From Fig. 5a, it can be seen that, at 0-deg incidence angle, the noise temperature of 6061-T6 aluminum

is 0.23 K, and the gain loss is 0.0034 dB. At 60-deg incidence angle, the noise temperature for parallel polarization increases rapidly and is nearly 0.5 K, and added-gain loss is close to 0.007 dB. The noise temperatures of the 6061-T6 aluminum mirror at 32 GHz seem high, but the same high value at 0-deg incidence angle was obtained through the use of approximate formulas given in [18]. As may be seen from Eq. (7), if six mirrors are involved, these noise temperatures for bare-metal mirrors alone are increased by about a factor of six, which is surprisingly high.

Excess noise temperatures and added-gain losses as functions of incidence angles at 32 GHz are shown in the Figs. 6 through 9 for four specific thickness layers of paints and primers, as follows:

(1) Figures 6a and 6b apply to the configuration of 0.127-mm (5-mil)-thick Triangle no. 6 paint and 0.0152-mm (0.6-mil)-thick zinc chromate primer on a 6061-T6 aluminum flat mirror.

(2) Figures 7a and 7b apply to the configuration of 0.0508-mm (2-mil)-thick 500FHR6 acrylic urethane-based paint with no primer on a flat 6061-T6 aluminum mirror.

(3) Figures 8a and 8b apply to the configuration of 0.127-mm (5-mil)-thick 18FHR6 paint and 0.0152-mm (0.6-mil)-thick 283 water-based primer on a flat 6061-T6 aluminum mirror.

(4) Figures 9a and 9b apply to the configuration of 0.0152-mm (0.6-mil)-thick zinc chromate primer on a flat 6061-T6 aluminum mirror.

Although not shown in Figs. 5 through 9, the noise temperatures and excess noise temperatures for circular polarization are the average of those for parallel and perpendicular polarizations [17]. Note that in Figs. 6 through 9 for parallel polarization, excess noise temperatures and added-gain losses increase rapidly with increasing incidence angles after 30 deg, while, for perpendicular polarization, the values decrease with increasing incidence angles.

Triangle no. 6 paint, 500FHR6 paint, 18FHR6 paint, and 283 primer are manufactured by Triangle Coatings, Inc., located in San Leandro, California. All of these named paints are thermal-diffusive white paints specially invented for the purpose of diffusing the heat generated when sunlight radiates on the metallic reflector surfaces. It is known that Triangle no. 6 paint's main ingredient is titanium dioxide, but the main ingredients of the other paints and primers manufactured by Triangle Coatings are not known to the authors. It is only known that 500FHR6 paint has an acrylic urethane base, while the 18FHR6 paint and 283 primer are water based.

The paint and primer thicknesses given above are based on thickness values in units of mils in the DSN paint specifications document [19]. It is easy to confuse metric units of mm (0.001 m) for English units of mils (0.001 inch). The formula for conversion from thickness t in mils to thickness t in mm is

$$t_{mm} = 0.0254 \times t_{mil}$$

In order to avoid confusion, the plots and tables will show both metric and English units for paint-layer thicknesses.

C. Plots as Functions of Paint and Primer Thickness

An alternate and perhaps better way of showing excess noise temperatures is to show excess noise temperatures as functions of paint- and primer-layer thicknesses at selected incidence angles. The selected incidence angles for this article are 0, 15, 30, 45, and 60 deg. For these plots, the excess noise temperatures will be shown for perpendicular, circular, and parallel polarizations.

Figures 10 through 14 are excess noise temperature plots presented as functions of thickness t at these incidence angles for Triangle no. 6 with a fixed zinc chromate primer-layer thickness of 0.0152 mm (0.6 mil). Note that when thickness t goes to zero, the noise temperature does not go to zero. The reason is that the residual noise temperature is due to the primer layer, which is not a function of thickness t.

Figures 15 through 19 are plots for 500FHR6 paint with no primer; Figs. 20 through 24 are plots for a 18FHR6 paint layer and a fixed 283 primer-layer thickness of 0.0152 mm (0.6 mil); and Figs. 25 through 29 are plots for zinc chromate primer only. For the parallel polarization case, high noise temperatures (about 2 K) occur for all cases of 0.254-mm (10-mil) thickness at 60-deg incidence angle.

For circular polarization, the excess noise temperatures are summarized in Table 2 for these paints (with fixed primer layers) for selected thicknesses of 0.0508 mm (2 mil), 0.127 mm (5 mil), 0.1778 mm (7 mil), and 0.254 mm (10 mil). Although not shown in the plots, Table 2 also gives the results for a very thick 0.381-mm (15-mil) layer for all paints and zinc chromate primer. Note that at this 0.381-mm thickness the excess noise temperatures for Triangle no. 6 paint cases are 1.5 K or greater at all incidence angles. This is important to show because, on some of the 70-m antenna reflector surfaces, repainting several times over 35 years may have built up paint layers to be much thicker than the DSN paint-thickness specifications without knowledge of the detrimental effects that excessive paint thickness have on noise temperature.

In Table 2, it can be seen that the 0.127-mm (5-mil) thickness for Triangle no. 6 paint and its primer layer thickness produce an excess noise temperature of 0.13 K at 30-deg incidence angle as compared with 0.03 K for 0.0508-mm (2-mil) 500FHR6 paint. These are of interest because they are the paint and primer thicknesses specified in the DSN antenna paint specification documents. Most of the higher noise temperature for the Triangle no. 6 paint configuration is due to the difference of a larger paint thickness and the existence of a primer layer. Note that the 18FHR6-paint with 283-primer-layer results are very similar to those for Triangle no. 6 paint with a zinc chromate primer layer. The excess noise temperatures of 500FHR6 paint with no primer are similar to the results produced by zinc chromate primer alone.

It was shown in Eq. (7) that excess noise temperature is additive for low-loss reflectors. Therefore, if there are six reflectors involved, such as the six BWG mirrors at DSS 13, each with only a zinc chromate primer layer, the total excess noise temperature will be about six times higher than the value for the single zinc chromate primer-painted mirror shown in Table 2. This kind of result was not known prior to this paint study.

D. Phase Plots

Depolarization due to paint on a reflector is a topic that often has been overlooked. A literature search revealed two articles [20,21] that discuss this topic. A complete study of depolarization is beyond the scope of this paint study, but some plots will be included in this article to show that future studies of depolarization effects need to be done.

For each set of curves in the following figures, the solid curves going upward from the 0-deg incidence-angle values are for parallel polarization, and the dashed curves going downward are for perpendicular polarization. Delta phase is equal to 180 deg minus the reflection coefficient phase. A flat reflector surface having no dissipative losses will have a delta phase value equal to zero. Comparisons of delta phase with and without paint and/or primer are given in these figures for nominal and worst-case paint- and primer-layer thicknesses on a flat 6061-T6 aluminum mirror. Only the values for perpendicular and parallel polarizations are shown. The results are grouped in four main paint-primer configurations as follows:

(1) Figures 30 and 31 are delta phase plots for 0.127-mm (5-mil)- and 0.254-mm (10-mil)-thick Triangle no. 6 paint, respectively, on a 0.0152-mm (0.6-mil) layer of zinc chromate primer.

(2) Figures 32 and 33 are delta phase plots for 0.0508-mm (2-mil)- and 0.254-mm (10-mil)-thick 500FHR6 acrylic urethane-based paint, respectively, with no primer.

(3) Figures 34 and 35 are delta phase plots for a 0.127-mm (5-mil)- and 0.254-mm (10-mil)-thick 18FHR6 paint layer, respectively, on a 0.0152-mm (0.6-mil) layer of 283 water-based primer.

(4) Figures 36 and 37 are delta phase plots for 0.0152-mm (0.6-mil)- and 0.254-mm (10-mil)-thick zinc chromate primer, respectively.

For all cases, the delta phase increases with increasing incidence angle for parallel polarization and decreases with increasing incidence angles for perpendicular polarization. Figure 30 shows that, for the 0.127-mm (5-mil)-thick Triangle no. 6 paint configuration of (1) above, the delta phase at 0-deg incidence angle is about 10 deg. Figure 32 shows that, for the 0.0508-mm (2-mil) 500FHR6 paint-thickness configuration, the delta phase at 0-deg incidence angle is about 4 deg. Similar observations and comparisons can be made for the 18FHR6 paint configuration of (3) above. For the thin zinc chromate primer layer of 0.0152-mm (0.6-mil) thickness, the delta phase at 0-deg incidence angle is only about 1 deg. When any of the paint and primer has a thickness of 0.254 mm (10 mil), the delta phase is about 20 deg.

It is not clear whether delta phase values of 4 to 10 deg or even 20 deg are detrimental to antenna performance, but these delta phase values might be equivalent to phase errors on main reflector or subreflector patterns. This is a subject area that needs to be investigated in future paint studies.

V. RECOMMENDATIONS AND CONCLUSION

It has been noted that it is essential to carefully assess the roles of surface paints and primers when one wants to characterize the ultimate performance of high performance reflector antennas. A thorough literature search revealed that not much has been reported on this very important engineering implementation topic. It was one of the main objectives of this feature article to provide a detailed study on the effects of paints and primers on the reflector antenna performance. In particular, as a case study, this paper presented excess noise temperature and added-gain loss data at 32 GHz for various combinations of paints and primers currently being studied for use on DSN (Deep Space Network) antenna reflector surfaces.

A suggested criterion for maximum allowable excess noise temperature due to paint and primer is 0.2 K at 32 GHz and 30-deg incidence angle for circular polarization. This criterion is selected on the basis that this excess noise temperature is a practical achievable value that does not cause significant degradation of DSN antennas performance at 32 GHz.

The value of DSN antennas is represented by their figures of merit [2], which are equal to G/T, where G is the receive system antenna gain and T is the receive system noise temperature. With these expensive DSN antenna systems operating at their current low system noise temperatures, the penalty is severe for any unnecessary increase of system noise temperature. DSN antennas operating at Goldstone at Ka-band (32 GHz) are expected in the future to have noise-temperature performances of about 50 K at 30-deg elevation angle (accounting for the effect of the atmosphere) [22]. Therefore, if system noise temperature is increased 1 K, the penalty to the DSN is to reduce the DSN antenna value by 2 percent per kelvin. Then, for the above suggested criterion, if paint and primer cause the system noise temperature to be increased a maximum of 0.2 K at 30-deg elevation angle, the penalty will be 0.4 percent. It should be pointed out that the actual total penalty will be slightly larger because, as was shown in this article, small but non-negligible losses due to paint and primer also cause a decrease of antenna gain. Therefore, every effort should be made to minimize paint and primer noise temperature and gain-loss contributions.

Based on the results presented in this article, a recommendation was made to use a 0.0509-mm (2-mil) or thinner layer of 500FHR6 paint with no primer on reflector surfaces for all new 34-m BWG antennas being built and for all existing 34-m and 70-m DSN antenna reflector surfaces that need repainting. This recommendation was incorporated into the updated DSN antenna paint specification document [19].

Paint on reflector surfaces can cause depolarization and associated degradations of antenna performance. Depolarization due to paint was not studied in this current study, but is an effect that should be investigated in the future. The results, methodologies and observations presented in this article are also applicable to other high performance reflector antenna systems.

References

1. C. D. Edwards, Jr., C. T. Stelzried, L. J. Deutsch, and L. Swanson, "NASA's Deep Space Telecommunications Road Map," *The Telecommunications and Mission Operations Progress Report 42-136, October-December 1998*, Jet Propulsion Laboratory, Pasadena, California, pp. 1–20, February 15, 1998.
http://tmo.jpl.nasa.gov/tmo/progress_report/42-136/136B.pdf

2. W. Rafferty, S. D. Slobin, C. T. Stelzried, and M. K. Sue, "Ground Antennas in NASA's Deep Space Communications," Invited Paper, *Proceedings of the IEEE (Special Issue on Radio Telescopes)*, pp. 636–646, May 1994.

3. T. Y. Otoshi, R. Cirillo, Jr., and J. Sosnowski, "Measurements of Complex Dielectric Constants of Paints and Primers for DSN Antennas: Part I," *The Telecommunications and Mission Operations Progress Report 42-138, April-June 1999*, Jet Propulsion Laboratory, Pasadena, California, pp. 1–13, August 15, 1999.
http://tmo.jpl.nasa.gov/tmo/progress_report/42-138/138F.pdf

4. T. Y. Otoshi, R. Cirillo, Jr., and J. Sosnowski, "Measurements of Complex Dielectric Constants of Paints and Primers for DSN Antennas: Part II," *The Telecommunications and Mission Operations Progress Report 42-139,* July-September 1999, Jet Propulsion Laboratory, Pasadena, California, pp. 1–7, November 15, 1999.
http://tmo.jpl.nasa.gov/tmo/progress_report/42-139/139G.pdf

5. D. A. Bathker, W. Veruttipong, T. Y. Otoshi, and P. W. Cramer, Jr., "Beam-Waveguide Antenna Performance Predictions with Comparisons to Experimental Results," *Microwave Theory and Techniques, Special Issue (Microwaves in Space)*, vol. MTT-40, no. 6, pp. 1274–1285, June 1992.

6. S. Ganchev, private communication, Hewlett-Packard, Englewood, Colorado, December 1999.

7. F. Ulaby, R. K. Moore, and A. K. Fung, *Microwave Remote Sensing*, Active and Passive, Appendix E, Dedham, Massachusetts: Artech House, pp. 2035, Equation 43b, 1986.

8. S. Gray, S. Ganchev, N. Qaddoumi, G. Beauregard, D. Radford, and R. Zoughi, "Porosity Level Estimation in Polymer Composites Using Microwaves," *Materials Evaluation*, pp. 404–408, March 1995.

9. A. R. Von Hipple, ed., *Dielectric Materials and Applications*, Cambridge, Massachusetts: MIT Press, 1954, fourth printing, 1966 (for TiO_2, see Tables of Dielectric Materials, p. 302).

10. *Reference Data For Radio Engineers*, fifth ed., International Telephone and Telegraph (ITT), New York: Howard W. Sams & Co., Inc., pp. 4–28, March 1968.

11. R. C. Clauss, private communication, Jet Propulsion Laboratory, Pasadena, CA, August 1989.

12. S. Ramo and J. R. Whinnery, *Fields and Waves in Modern Radio*, second ed., New York: John Wiley and Sons, p. 320, Eq. 9, 1953.

13. T. Battilana, "Ensure Uniformity When Specifying Paint for Reflectors," *Microwaves and RF*, p. 113–122, March 1988. Correction in *Microwaves and RF*, p. 13, June 1988.

14. W. B. Weir, "Automatic Measurement of Complex Dielectric Constant and Permeability at Microwave Frequencies," *Proceedings of the IEEE*, vol. 62, no. 1, pp. 33–36, January 1974.

15. Hewlett Packard, "Materials Measurement: Measuring the Dielectric Constant of Solids With the HP 8510 Network Analyzer," Hewlett Packard Product Note 8510-3, August 1, 1985.

16. H.-P. Ip and Y. Rahmat-Samii, "Analysis and Characterization of Multilayered Reflector Antennas: Rain/Snow Accumulation and Deployable Membrane," *IEEE Trans. on Antennas and Propagation*, vol. 46, no. 11, pp. 1593–1605, November 1998.

17. T. Y. Otoshi and C. Yeh, "Noise Temperature of a Lossy Flat-Plate Reflector for the Elliptically Polarized Wave Case," *IEEE Trans. on Microwave Theory and Techniques* (accepted for publication April 2000).

18. T. Y. Otoshi and M. M. Franco, "The Electrical Conductivities of Steel and Other Candidate Material for Shrouds in a Beam-Waveguide Antenna System," *IEEE Trans. on Instrumentation and Measurement*, vol. IM-45, no. 1, pp. 77–83, February 1996. Correction in IEEE Trans. on Instrumentation and Measurement, vol. IM-45, no. 4, p. 839, August 1996.

19. T. C. Sink, private communication, Jet Propulsion Laboratory, Pasadena, CA, September 1999.

20. T. S. Chu and R. A. Semplak, "A Note on Painted Reflecting Surfaces," *IEEE Trans. on Ant and Prop.*, vol. AP-24, no. 1, pp. 99–101, January 1976.

21. K. K. Chen and A. R. Raab, "Some Aspects of Beam Waveguide Design," *IEE Proc.*, vol. 129, pt. H, no. 4, pp. 203–221, August 1982.

22. C. T. Stelzried, private communication, Jet Propulsion Laboratory, Pasadena, CA, December 29, 1999.

Captions for Figures

Figure 1. The 34-m-diameter BWG antenna at DSS 13, showing painted solid and perforated reflector surfaces.

Figure 2. The 34-m-diameter BWG antenna at DSS13, showing the painted subreflector and subreflector support legs. Note author T. Otoshi standing on platform above subreflector.

Figure 3. The 34-m-diameter BWG antenna at DSS13, showing one of the BWG mirrors (in the subterranean room) coated with zinc chromate primer.

Figure 4. Schematic configuration of various cases studied by changing the incidence angle, paint and primer thicknesses, and material properties per Tables 1 and 2.

Figure 5. (a) The total noise temperature; (b) the gain loss of a flat 6061-T6 aluminum mirror at 32 GHz.

Figure 6. (a) The total excess noise temperature contribution; (b) the added-gain loss at 32 GHz due to 0.127-mm (5-mil)-thick Triangle no. 6 paint and 0.0152-mm (0.6-mil)-thick zinc chromate primer on a flat 6061-T6 aluminum mirror.

Figure 7. (a) The total excess noise temperature; (b) the added gain loss at 32 GHz due to 0.0508-mm (2.0-mil)-thick 500FHR6 paint and no primer on a flat 6061-T6 aluminum mirror.

Figure 8. (a) The total excess noise-temperature contribution; (b) the added-gain loss at 32 GHz due to 0.127-mm (5.0-mil)-thick 18FHR6 paint and 0.0152-mm (0.6-mil)-thick 283 primer on a flat 6061-T6 aluminum mirror.

Figure 9. (a) The excess noise-temperature contribution; (b) the added-gain loss at 32 GHz due to 0.0152-mm (0.6-mil)-thick zinc chromate primer on a flat 6061-T6 aluminum mirror.

Figure 10. The total excess noise temperature due to a Triangle no. 6 paint layer of thickness t and a fixed zinc chromate primer-layer thickness of 0.0152 mm (0.6 mil) at 0-deg incidence angle and 32 GHz. The single curve applies to parallel, circular, and perpendicular polarizations.

Figure 11. The total excess noise temperature due to a Triangle no. 6 paint layer of thickness *t* and a fixed zinc chromate primer-layer thickness of 0.0152 mm (0.6 mil) at 15-deg incidence angle and 32 GHz. The middle curve is the average of parallel and perpendicular polarization excess noise temperatures and applies to circular polarization.

Figure 12. The total excess noise temperature due to a Triangle no. 6 paint layer of thickness *t* and a fixed zinc chromate primer-layer thickness of 0.0152 mm (0.6 mil) at 30-deg incidence angle and 32 GHz.

Figure 13. The total excess noise temperature due to a Triangle no. 6 paint layer of thickness *t* and a fixed zinc chromate primer-layer thickness of 0.0152 mm (0.6 mil) at 45-deg incidence angle and 32 GHz.

Figure 14. The excess noise temperature due to a Triangle no. 6 paint layer of thickness *t* and a fixed zinc chromate primer-layer thickness of 0.0152 mm (0.6 mil) at 60-deg incidence angle and 32 GHz.

Figure 15. The excess noise temperature due to a 500FHR6 paint layer of thickness t and no primer layer at 0-deg incidence angle and 32 GHz. The single curve applies to parallel, circular, and perpendicular polarizations.

Figure 16. The excess noise temperature due to a 500FHR6 paint layer of thickness t and no primer layer at 15-deg incidence angle and 32 GHz. The middle curve is the average of parallel and perpendicular polarization excess noise temperatures and applies to circular polarization.

Figure 17. The excess noise temperature due to a 500FHR6 paint layer of thickness t and no primer layer at 30-deg incidence angle and 32 GHz.

Figure 18. The excess noise temperature due to a 500FHR6 paint layer of thickness t and no primer layer at 45-deg incidence angle and 32 GHz.

Figure 19. The excess noise temperature due to a 500FHR6 paint layer of thickness t and no primer layer at 60-deg incidence angle and 32 GHz.

Figure 20. The total excess noise temperature due to a 18FHR6 paint layer of thickness t and a fixed 283 primer-layer thickness of 0.0152 mm (0.6 mil) at 0-deg incidence angle and 32 GHz. The single curve applies to parallel, circular, and perpendicular polarizations.

Figure 21. The total excess noise temperature due to a 18FHR6 paint layer of thickness t and a fixed 283 primer-layer thickness of 0.0152 mm (0.6 mil) at 15-deg incidence angle and 32 GHz. The middle curve is the average of parallel and perpendicular polarization excess noise temperatures and applies to circular polarization.

Figure 22. The total excess noise temperature due to a 18FHR6 paint layer of thickness t and a fixed 283 primer-layer thickness of 0.0152 mm (0.6 mil) at 30-deg incidence angle and 32 GHz.

Figure 23. The total excess noise temperature due to a 18FHR6 paint layer of thickness t and a fixed 283 primer-layer thickness of 0.0152 mm (0.6 mil) at 45-deg incidence angle and 32 GHz.

Figure 24. The total excess noise temperature due to a 18FHR6 paint layer of thickness t and a fixed 283 primer-layer thickness of 0.0152 mm (0.6 mil) at 60-deg incidence angle and 32 GHz.

Figure 25. The excess noise temperature due zinc chromate primer layer of thickness t at 0-deg incidence angle and 32 GHz. The single curve applies to parallel, circular, and perpendicular polarizations.

Figure 26. The excess noise temperature due zinc chromate primer layer of thickness t at 15-deg incidence angle and 32 GHz. The middle curve is the average of parallel and perpendicular polarization excess noise temperatures and applies to circular polarization.

Figure 27. The excess noise temperature due to a zinc chromate primer layer of thickness t at 30-deg incidence angle and 32 GHz.

Figure 28. The excess noise temperature due to a zinc chromate paint layer of thickness t at 45-deg incidence angle and 32 GHz.

Figure 29. The excess noise temperature due to a zinc chromate primer layer of thickness t at 60-deg incidence angle and 32 GHz.

Figure 30. A comparison of delta phase with and without 0.127-mm (5-mil)-thick Triangle no. 6 paint and 0.0152-mm (0.6-mil)-thick zinc chromate primer on a flat 6061-T6 aluminum mirror.

Figure 31. A comparison of delta phase with and without 0.254-mm (10-mil)-thick Triangle no. 6 paint and 0.0152-mm (0.6-mil)-thick zinc chromate primer on a flat 6061-T6 aluminum mirror.

Figure 32. A comparison of delta phase with and without 0.0508-mm (2-mil)-thick 500FHR6 acrylic urethane-based paint on a flat 6061-T6 aluminum mirror.

Figure 33. A comparison of delta phase with and without 0.254-mm (10-mil)-thick 500FHR6 paint with no primer on a flat 6061-T6 aluminum mirror.

Figure 34. A comparison of delta phase with and without 0.127-mm (5-mil)-thick 18FHR6 water-based paint and 0.0152-mm (0.6-mil)-thick 283 water-based primer on a flat 6061-T6 aluminum mirror.

Figure 35. A comparison of delta phase with and without 0.254-mm (10-mil)-thick 18FHR6 water-based paint and 0.0152-mm (0.6-mil)-thick 283 water-based primer on a flat 6061-T6 aluminum mirror.

Figure 36. A comparison of delta phase with and without 0.0152-mm (0.6-mil)-thick zinc chromate primer on a flat 6061-T6 aluminum mirror.

Figure 37. A comparison of delta phase with and without 0.254-mm (10-mil)-thick zinc chromate primer on a flat 6061-T6 aluminum mirror.

Table 1. Average measured paint/primer complex relative dielectric constant values in the 32-GHz frequency region.[a]

Paint or primer	Frequency, GHz	ε_r'	ε_r''	Loss tangent	Electrical conductivity, mhos/m
Triangle no. 6 paint	31-33	5.908 0.019 SD	0.148 0.014 SD	0.025 0.002 SD	0.2631
Zinc chromate primer	32-34	4.361 0.001 SD	0.0949 0. 0001 SD	0.0218 0.00003 SD	0.1687
18FHR6 Paint	31-33	5.275 0.012 SD	0.153 0.008 SD	0.0291 0.0014 SD	0.2720
283 Primer	31-33	3.300 0.001 SD	0.121 0.001 SD	0.0367 0.0003 SD	0.2151
500FHR6 Paint	31-33	4.691 0.001 SD	0.111 0.001 SD	0.0236 0.0002 SD	0.1973

[a]SD = the standard deviation of the average based on the number of frequency points.

Complex relative dielectric constant = $\left(\varepsilon_r' - j\,\varepsilon_r''\right)$.

Loss tangent = $\varepsilon_r'' / \varepsilon_r'$.

Electrical conductivity = $\varepsilon_r'' \times$ Frequency (GHz)/18. For this table, Frequency (GHz) = 32.0 was used.

Table 2. Comparison of excess ENTs for circular polarization at 32 GHz for four different configurations of paint and primer layers at selected thicknesses and incidence angles.

Thickness t, mm	Thickness t, mil	Triangle no. 6 configuration[a] ENT, K	500FHR6 configuation[b] ENT,K	18FHR6 configuation[c] ENT, K	Zinc chromate configuation[d] ENT, K
		0-deg incidence angle			
0.0508	2	0.008	0.003	0.007	0.002
0.1270	5	0.063	0.034	0.063	0.029
0.1778	7	0.154	0.089	0.154	0.077
0.2540	10	0.426	0.259	0.426	0.221
0.3810	15	1.523	0.932	1.498	0.786
		15-deg incidence angle			
0.0508	2	0.015	0.010	0.019	0.009
0.1270	5	0.079	0.051	0.086	0.046
0.1778	7	0.176	0.113	0.185	0.100
0.2540	10	0.455	0.292	0.466	0.254
0.3810	15	1.557	0.976	1.548	0.830
		30-deg incidence angle			
0.0508	2	0.040	0.032	0.058	0.031
0.1270	5	0.131	0.105	0.160	0.100
0.1778	7	0.245	0.188	0.281	0.175
0.2540	10	0.548	0.397	0.594	0.358
0.3810	15	1.670	1.118	1.708	0.972
		45-deg incidence angle			
0.0508	2	0.088	0.074	0.131	0.073
0.1270	5	0.231	0.210	0.301	0.203
0.1778	7	0.380	0.333	0.467	0.318
0.2540	10	0.731	0.599	0.842	0.557
0.3810	15	1.899	1.392	2.023	1.244
		60-deg incidence angle			
0.0508	2	0.178	0.153	0.270	0.151
0.1270	5	0.420	0.405	0.566	0.396
0.1778	7	0.633	0.603	0.814	0.584
0.2540	10	1.072	0.971	1.299	0.923
0.3810	15	2.308	1.876	2.579	1.723

[a]Triangle no. 6 paint and a 0.0152-mm (0.6-mil)-thick layer of zinc chromate primer.

[b]500FHR6 paint only.

[c]18FHR6 paint and 0.0152-mm (0.6-mil)-thick layer of 283 primer.

[d]Zinc chromate primer only.

Figure 1. The 34-m-diameter BWG antenna at DSS 13, showing painted solid and perforated reflector surfaces.

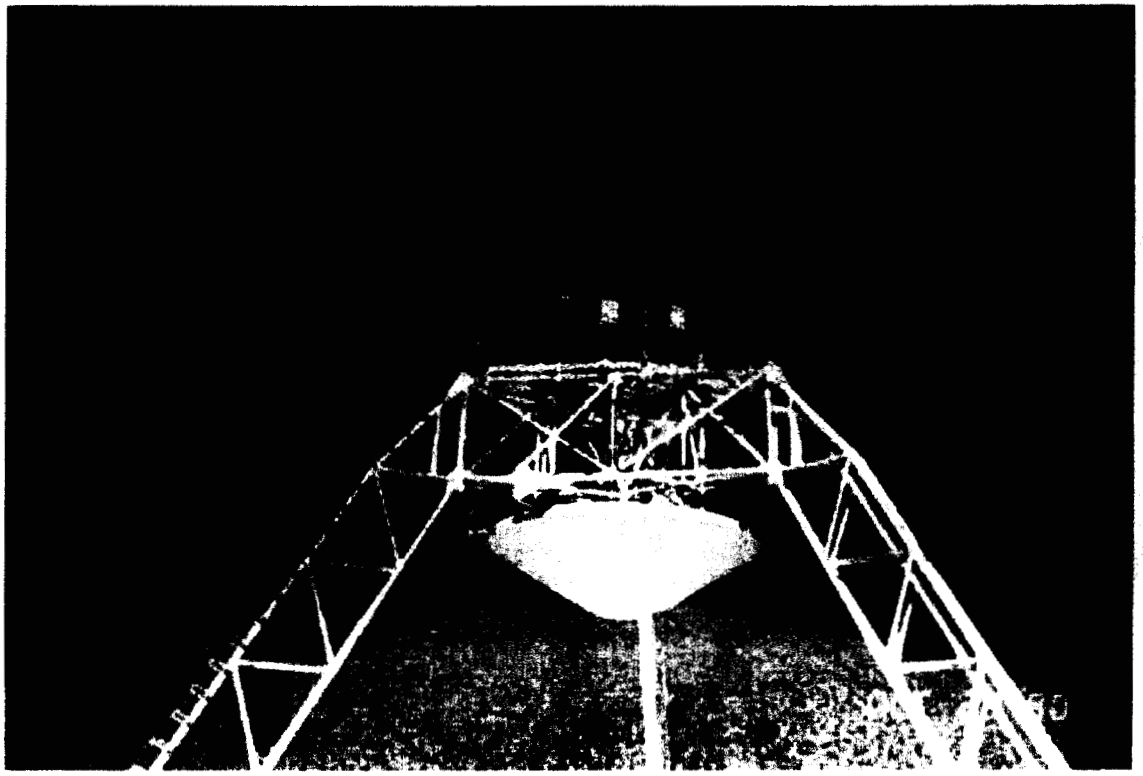

Figure 2. The 34-m-diameter BWG antenna at DSS13, showing the painted subreflector and subreflector support legs. Note author T. Otoshi standing on platform above subreflector.

Figure 3. The 34-m-diameter BWG antenna at DSS13, showing one of the BWG mirrors (in the subterranean room) coated with zinc chromate primer.

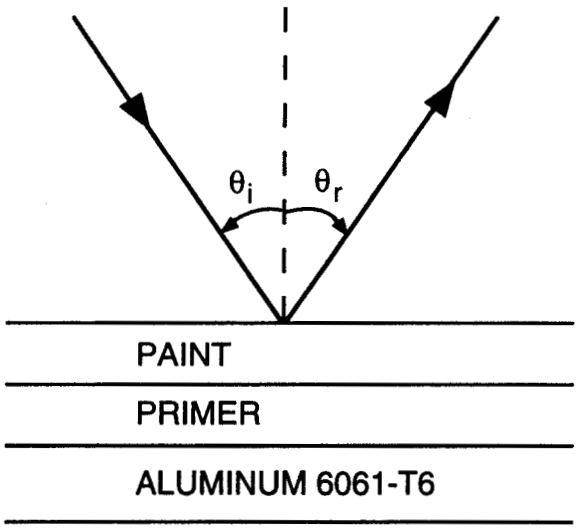

Figure 4. Schematic configuration of various cases studied by changing the incidence angle, paint and primer thicknesses, and material properties per Tables 1 and 2.

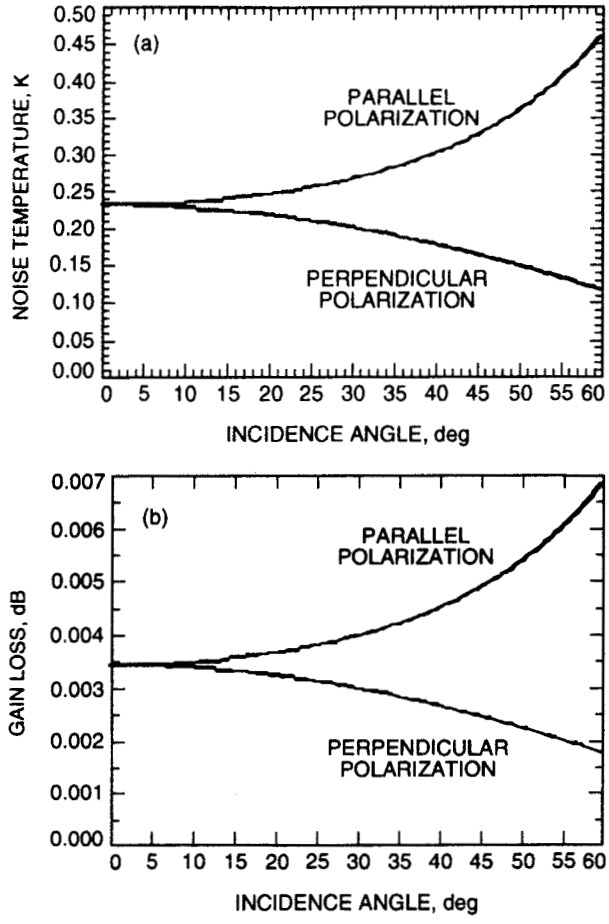

Figure 5. (a) The total noise temperature; (b) the gain loss of a flat 6061-T6 aluminum mirror at 32 GHz.

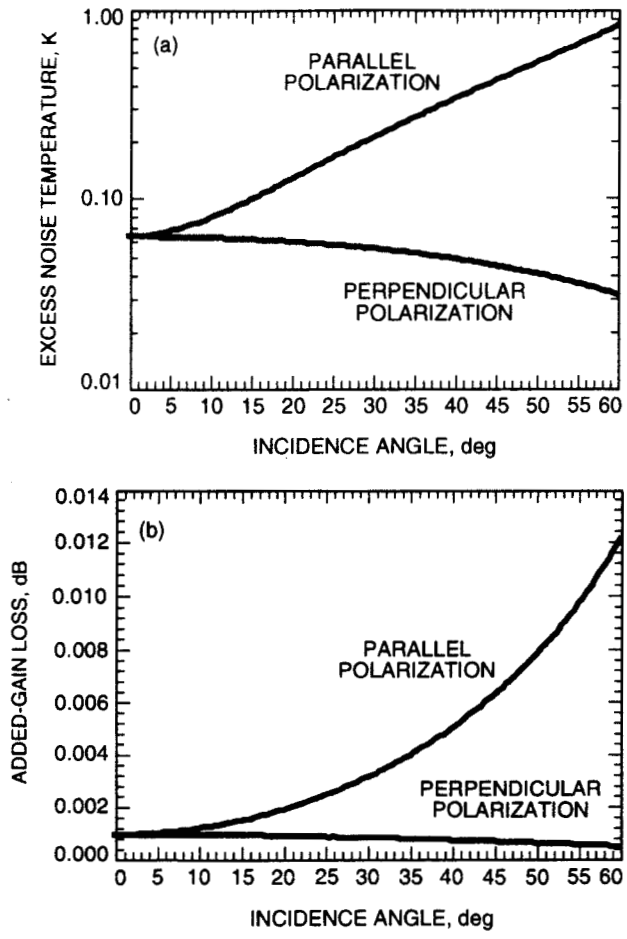

Figure 6. (a) The total excess noise temperature contribution; (b) the added-gain loss at 32 GHz due to 0.127-mm (5-mil)-thick Triangle no. 6 paint and 0.0152-mm (0.6-mil)-thick zinc chromate primer on a flat 6061-T6 aluminum mirror.

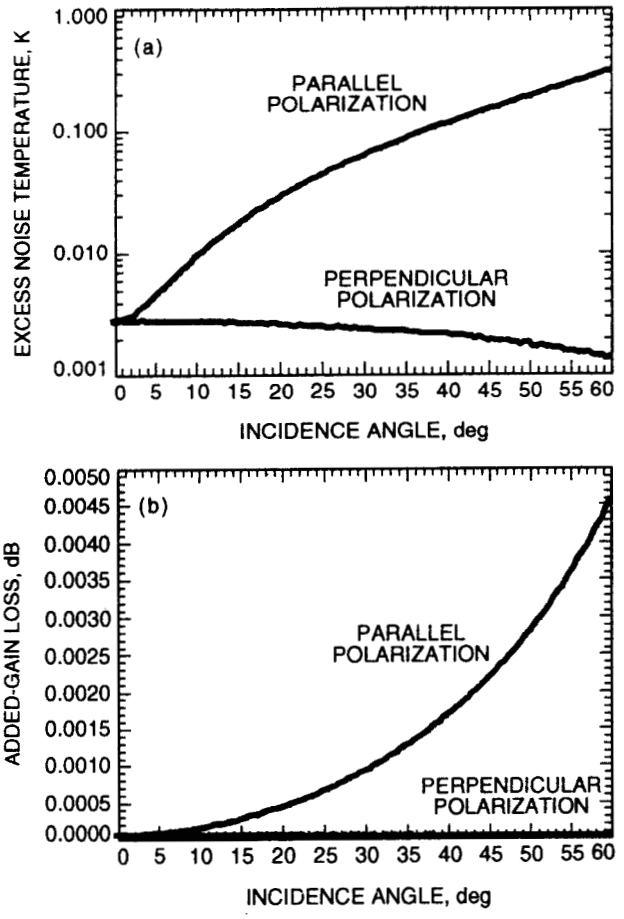

Figure 7. (a) The total excess noise temperature; (b) the added gain loss at 32 GHz due to 0.0508-mm (2.0-mil)-thick 500FHR6 paint and no primer on a flat 6061-T6 aluminum mirror.

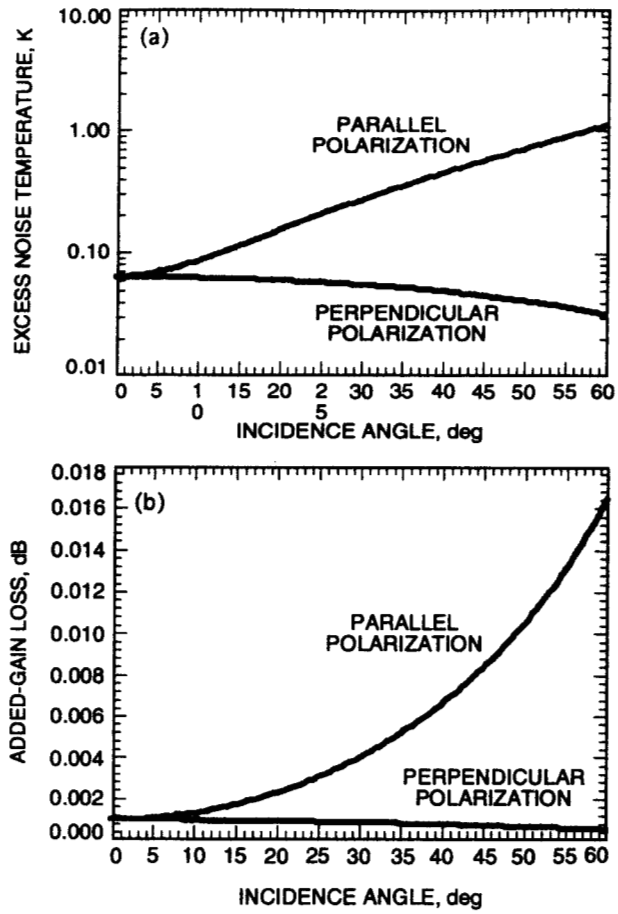

Figure 8. (a) The total excess noise-temperature contribution; (b) the added-gain loss at 32 GHz due to 0.127-mm (5.0-mil)-thick 18FHR6 paint and 0.0152-mm (0.6-mil)-thick 283 primer on a flat 6061-T6 aluminum mirror.

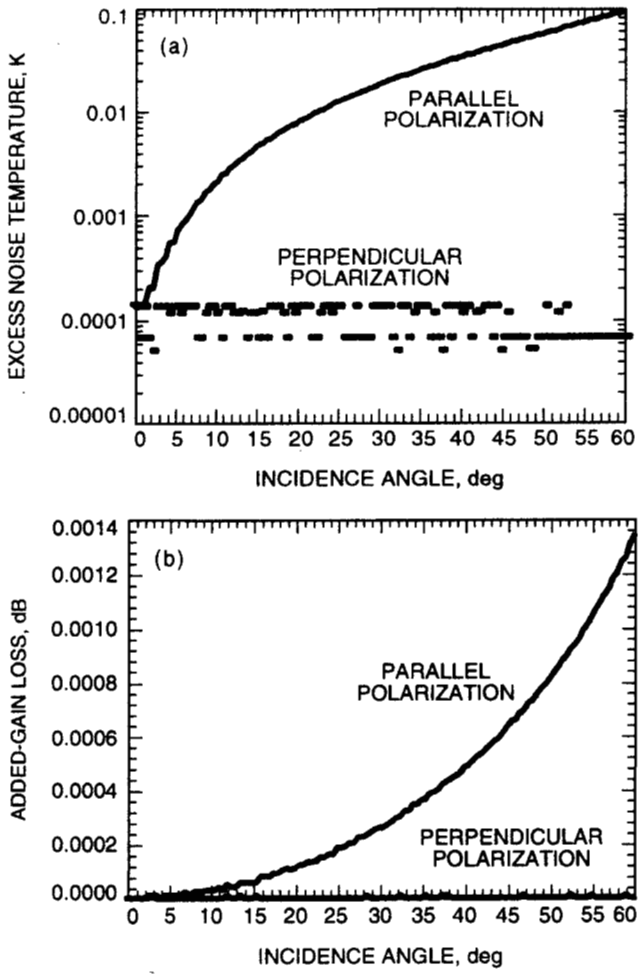

Figure 9. (a) The excess noise-temperature contribution; (b) the added-gain loss at 32 GHz due to 0.0152-mm (0.6-mil)-thick zinc chromate primer on a flat 6061-T6 aluminum mirror.

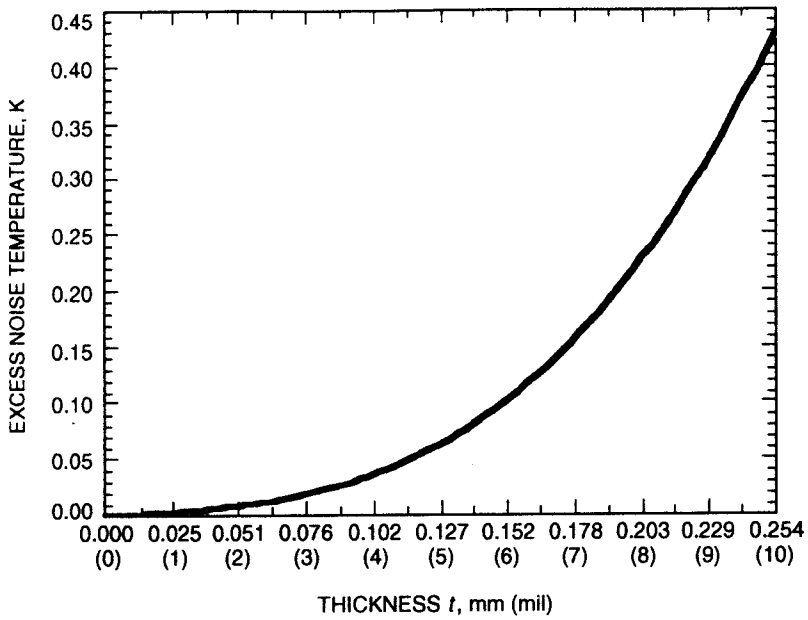

Figure 10. The total excess noise temperature due to a Triangle no. 6 paint layer of thickness t and a fixed zinc chromate primer-layer thickness of 0.0152 mm (0.6 mil) at 0-deg incidence angle and 32 GHz. The single curve applies to parallel, circular, and perpendicular polarizations.

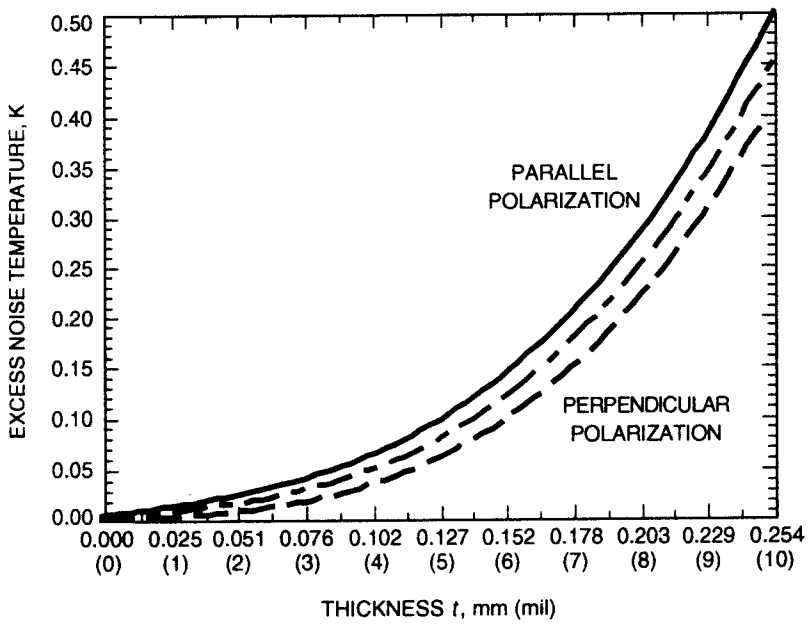

Figure 11. The total excess noise temperature due to a Triangle no. 6 paint layer of thickness t and a fixed zinc chromate primer-layer thickness of 0.0152 mm (0.6 mil) at 15-deg incidence angle and 32 GHz. The middle curve is the average of parallel and perpendicular polarization excess noise temperatures and applies to circular polarization.

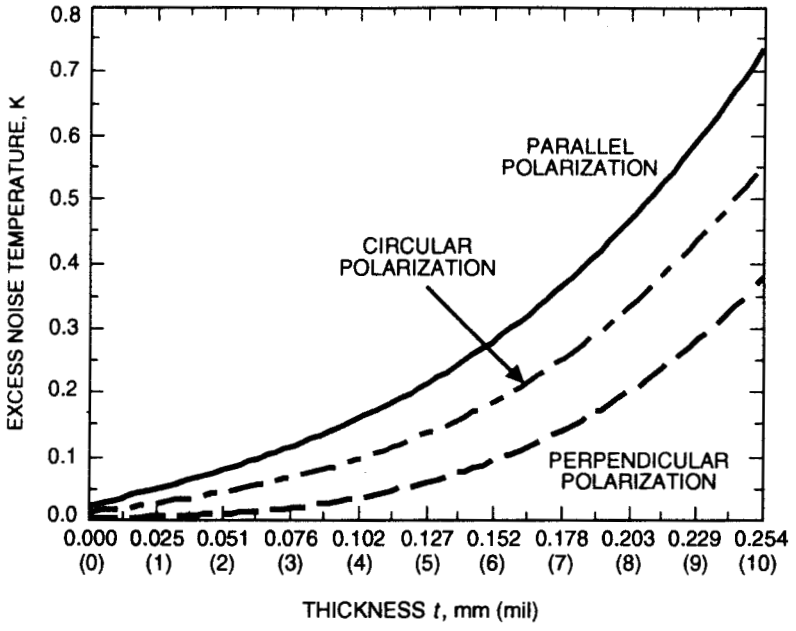

Figure 12. The total excess noise temperature due to a Triangle no. 6 paint layer of thickness t and a fixed zinc chromate primer-layer thickness of 0.0152 mm (0.6 mil) at 30-deg incidence angle and 32 GHz.

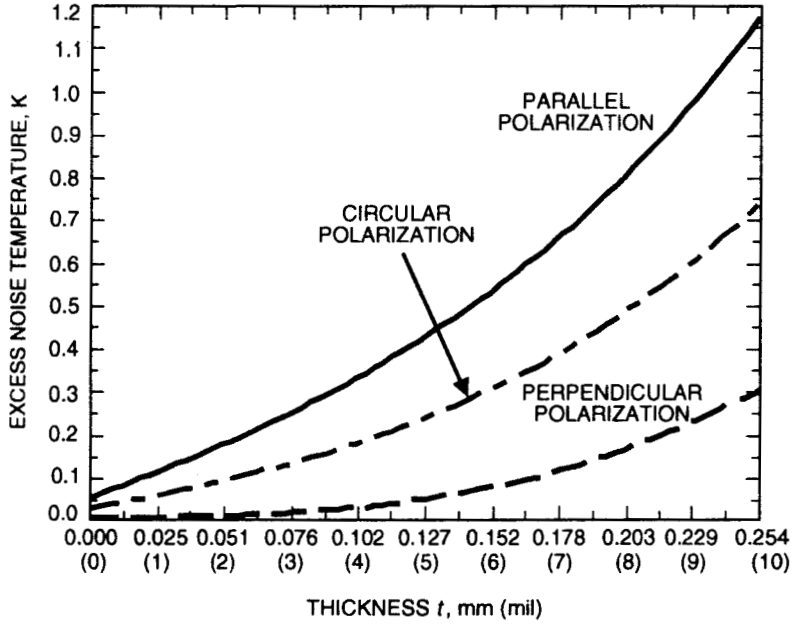

Figure 13. The total excess noise temperature due to a Triangle no. 6 paint layer of thickness t and a fixed zinc chromate primer-layer thickness of 0.0152 mm (0.6 mil) at 45-deg incidence angle and 32 GHz.

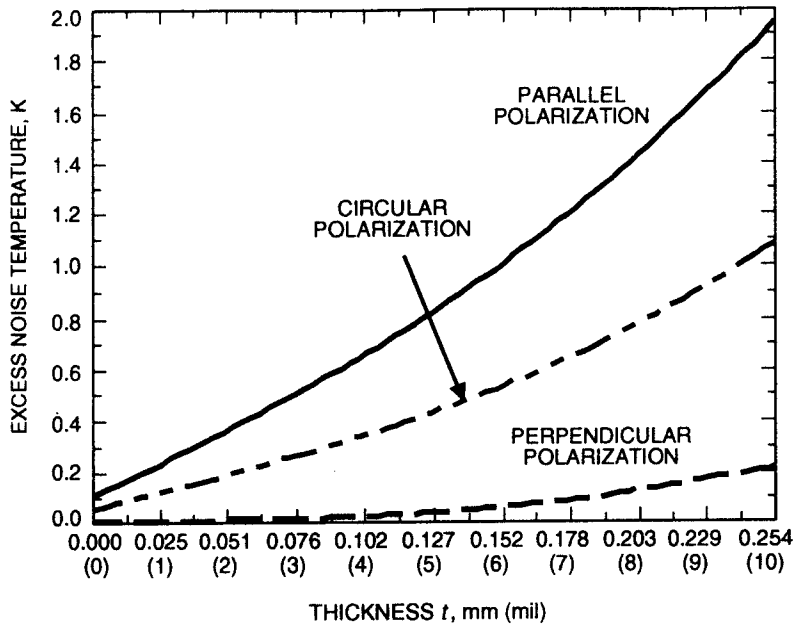

Figure 14. The total excess noise temperature due to a Triangle no. 6 paint layer of thickness t and a fixed zinc chromate primer-layer thickness of 0.0152 mm (0.6 mil) at 60-deg incidence angle and 32 GHz.

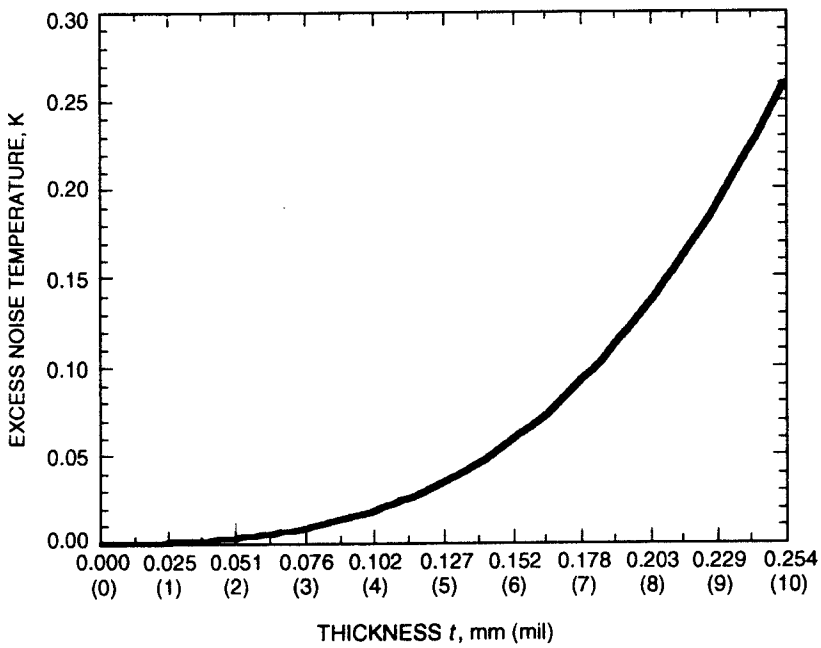

Figure 15. The excess noise temperature due to a 500FHR6 paint layer of thickness t and no primer layer at 0-deg incidence angle and 32 GHz. The single curve applies to parallel, circular, and perpendicular polarizations.

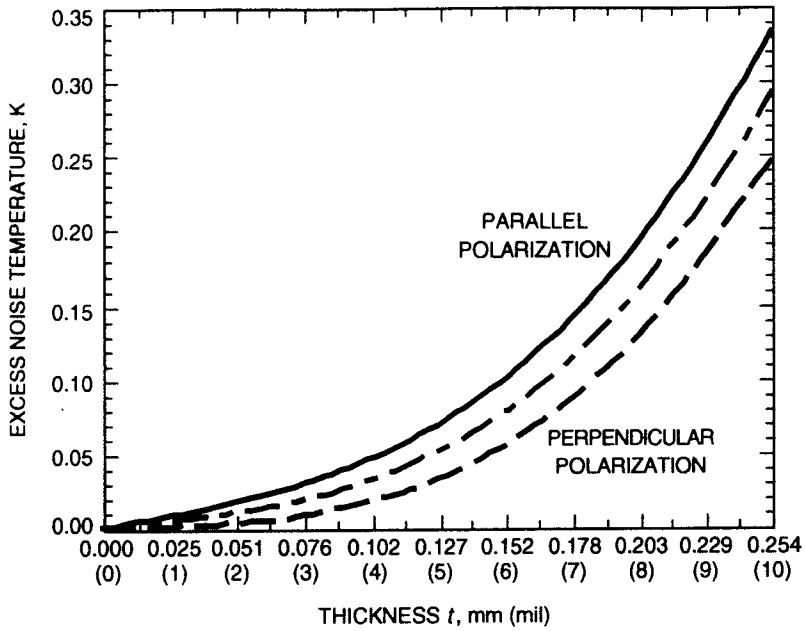

Figure 16. The excess noise temperature due to a 500FHR6 paint layer of thickness t and no primer layer at 15-deg incidence angle and 32 GHz. The middle curve is the average of parallel and perpendicular polarization excess noise temperatures and applies to circular polarization.

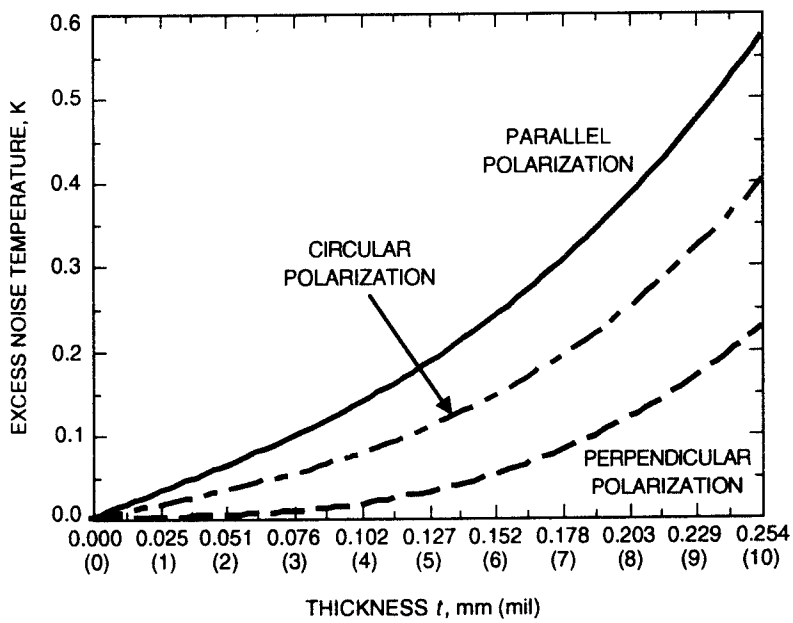

Figure 17. The excess noise temperature due to a 500FHR6 paint layer of thickness t and no primer layer at 30-deg incidence angle and 32 GHz.

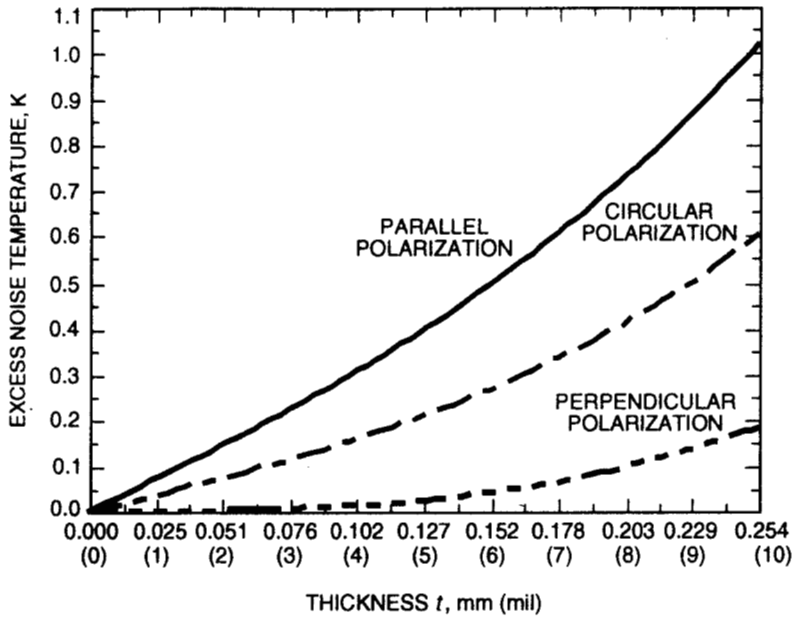

Figure 18. The excess noise temperature due to a 500FHR6 paint layer of thickness t and no primer layer at 45-deg incidence angle and 32 GHz.

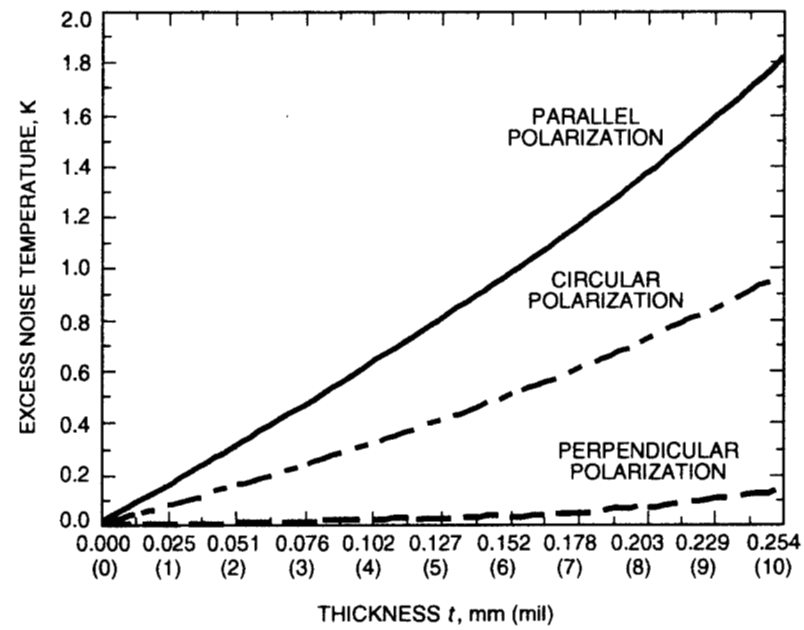

Figure 19. The excess noise temperature due to a 500FHR6 paint layer of thickness t and no primer layer at 60-deg incidence angle and 32 GHz.

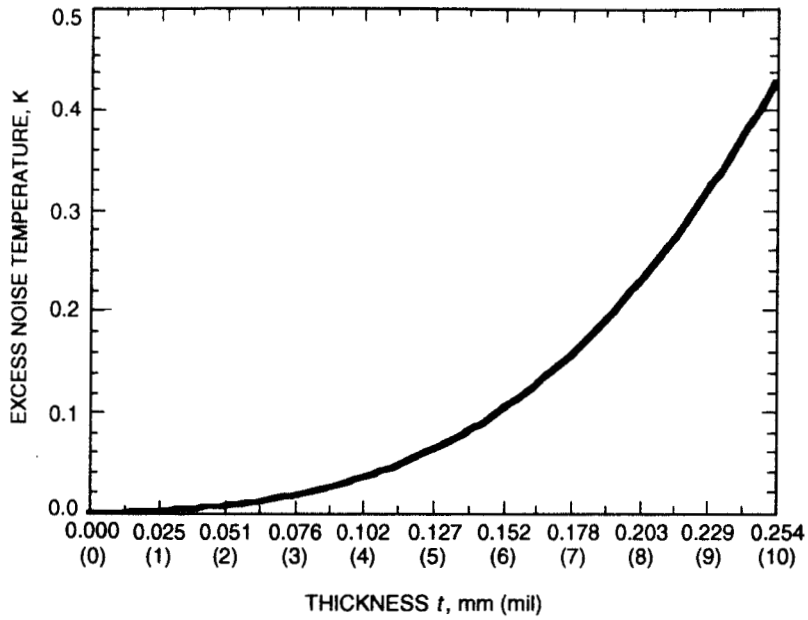

Figure 20. The total excess noise temperature due to a 18FHR6 paint layer of thickness t and a fixed 283 primer-layer thickness of 0.0152 mm (0.6 mil) at 0-deg incidence angle and 32 GHz. The single curve applies to parallel, circular, and perpendicular polarizations.

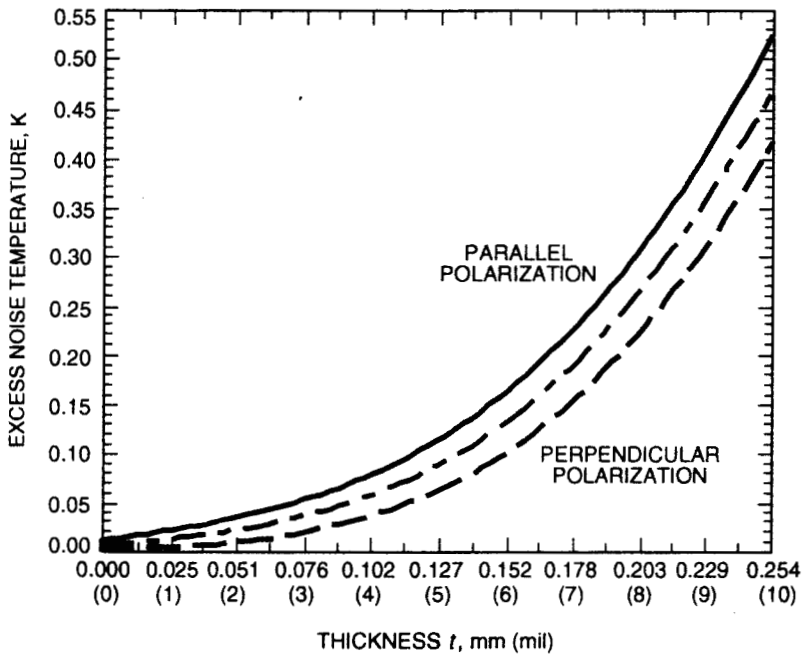

Figure 21. The total excess noise temperature due to a 18FHR6 paint layer of thickness t and a fixed 283 primer-layer thickness of 0.0152 mm (0.6 mil) at 15-deg incidence angle and 32 GHz. The middle curve is the average of parallel and perpendicular polarization

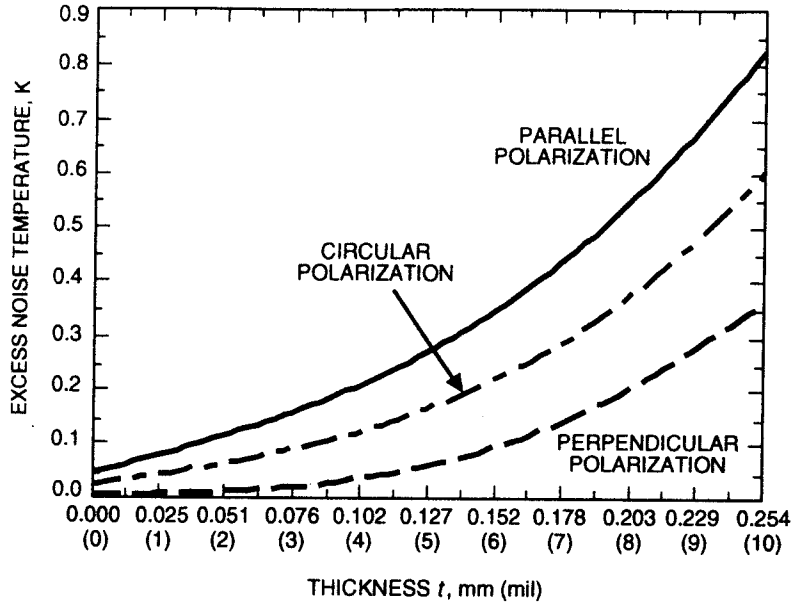

Figure 22. The total excess noise temperature due to a 18FHR6 paint layer of thickness t and a fixed 283 primer-layer thickness of 0.0152 mm (0.6 mil) at 30-deg incidence angle and 32 GHz.

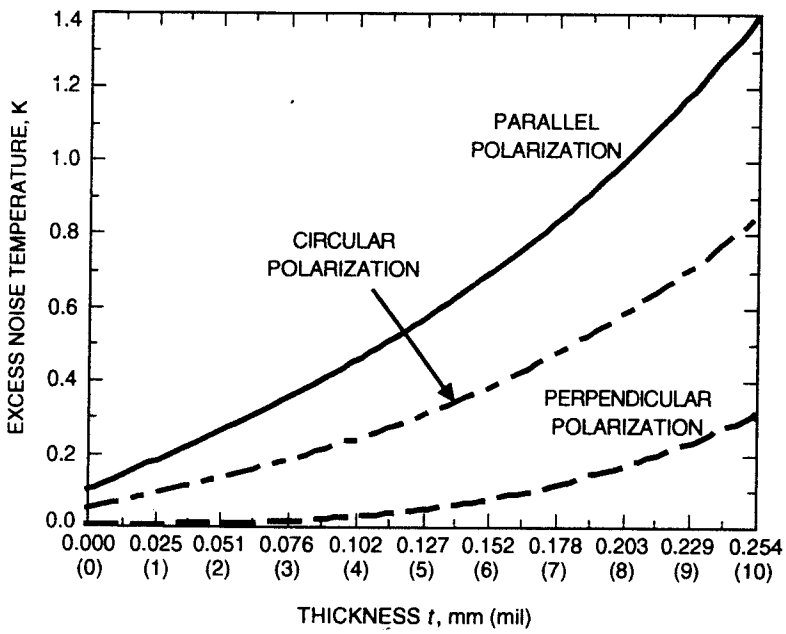

Figure 23. The total excess noise temperature due to a 18FHR6 paint layer of thickness t and a fixed 283 primer-layer thickness of 0.0152 mm (0.6 mil) at 45-deg incidence angle and 32 GHz.

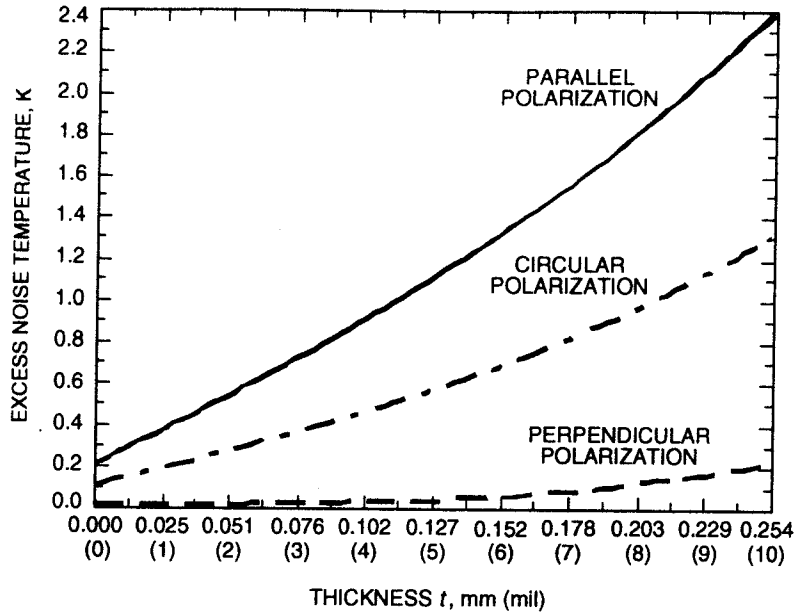

Figure 24. The total excess noise temperature due to a 18FHR6 paint layer of thickness t and a fixed 283 primer-layer thickness of 0.0152 mm (0.6 mil) at 60-deg incidence angle and 32 GHz.

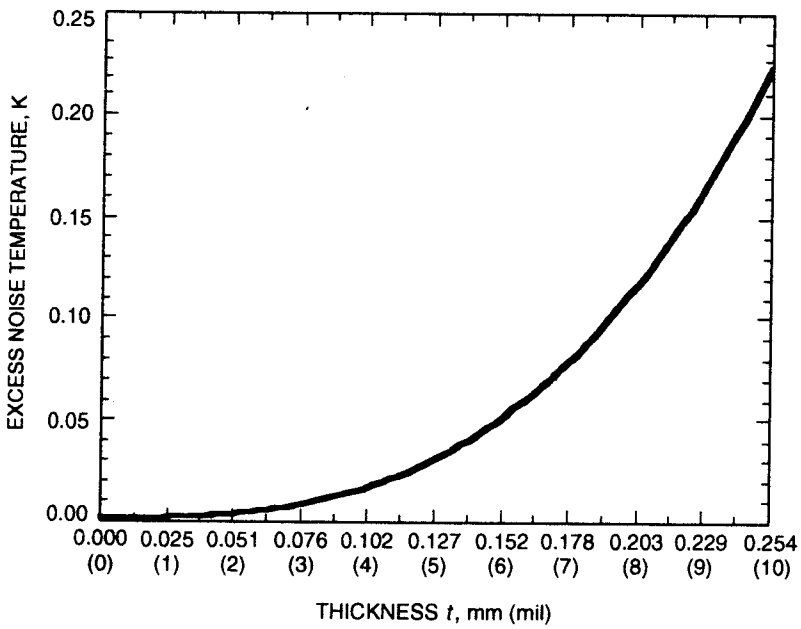

Figure 25. The excess noise temperature due to a zinc chromate primer layer of thickness t at 0-deg incidence angle and 32 GHz. The single curve applies to parallel, circular, and perpendicular polarizations.

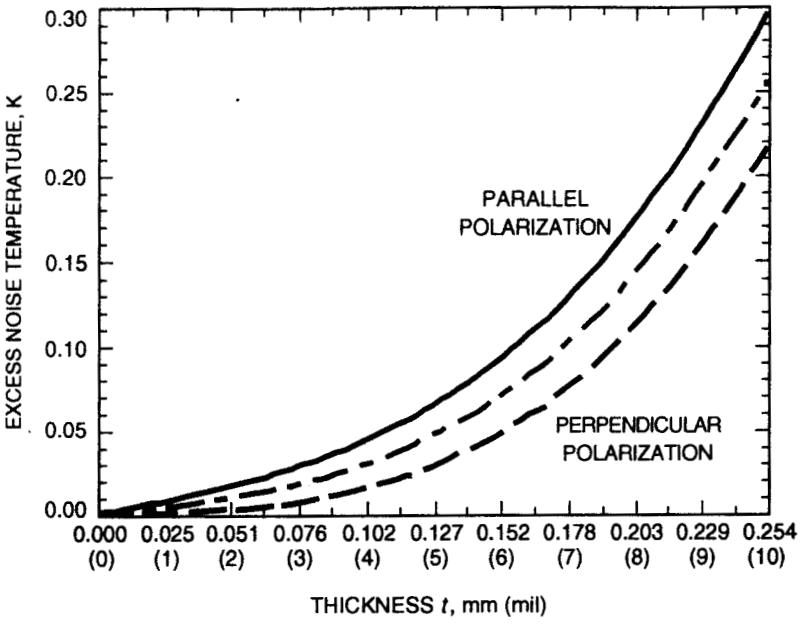

Figure 26. The excess noise temperature due to a zinc chromate primer layer of thickness t at 15-deg incidence angle and 32 GHz. The middle curve is the average of parallel and perpendicular polarization excess noise temperatures and applies to circular polarization.

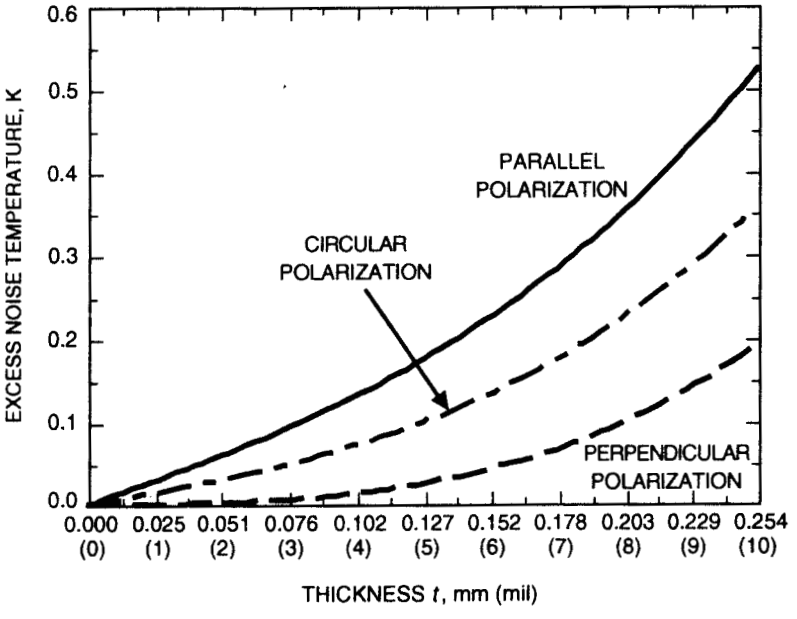

Figure 27. The excess noise temperature due to a zinc chromate primer layer of thickness t at 30-deg incidence angle and 32 GHz.

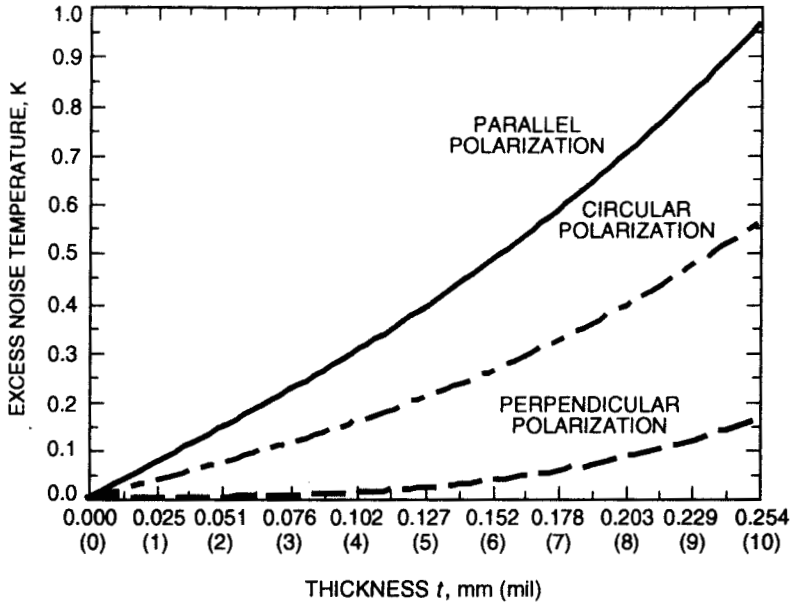

Figure 28. The excess noise temperature due to a zinc chromate paint layer of thickness t at 45-deg incidence angle and 32 GHz.

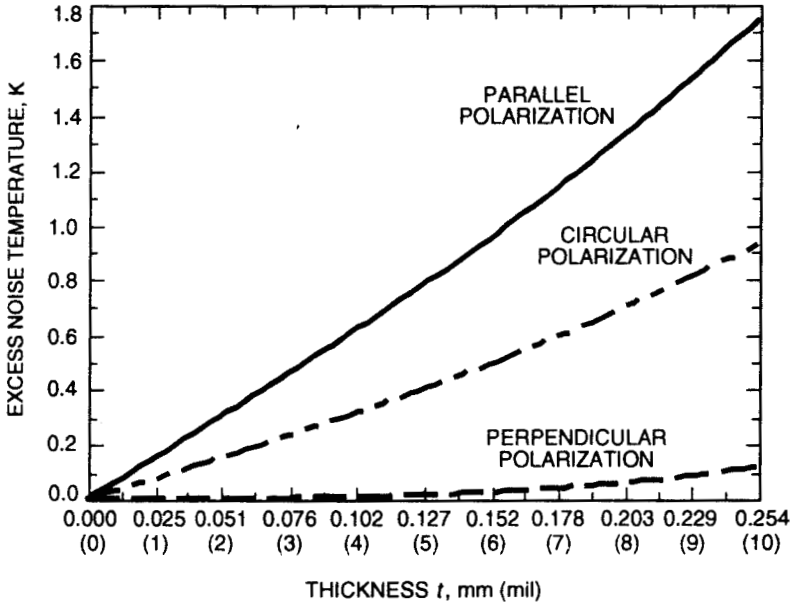

Figure 29. The excess noise temperature due to a zinc chromate primer layer of thickness t at 60-deg incidence angle and 32 GHz.

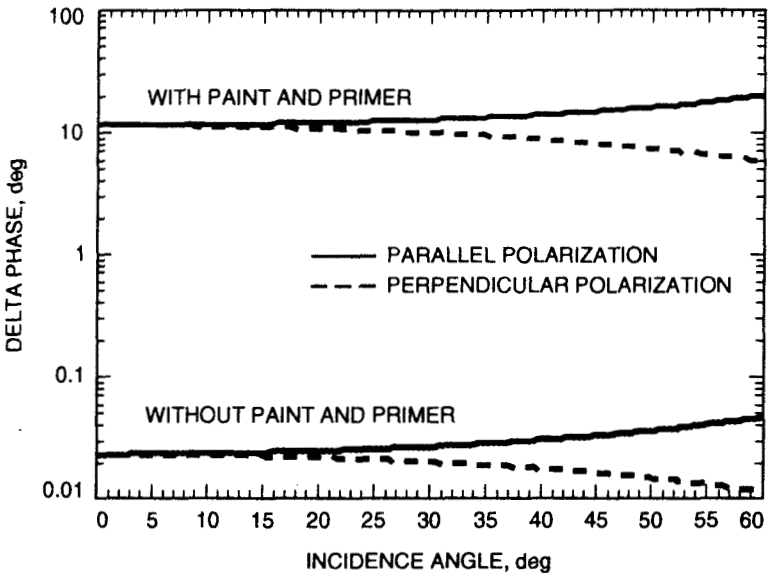

Figure 30. A comparison of delta phase with and without 0.127-mm (5-mil)-thick Triangle no. 6 paint and 0.0152-mm (0.6-mil)-thick zinc chromate primer on a flat 6061-T6 aluminum mirror.

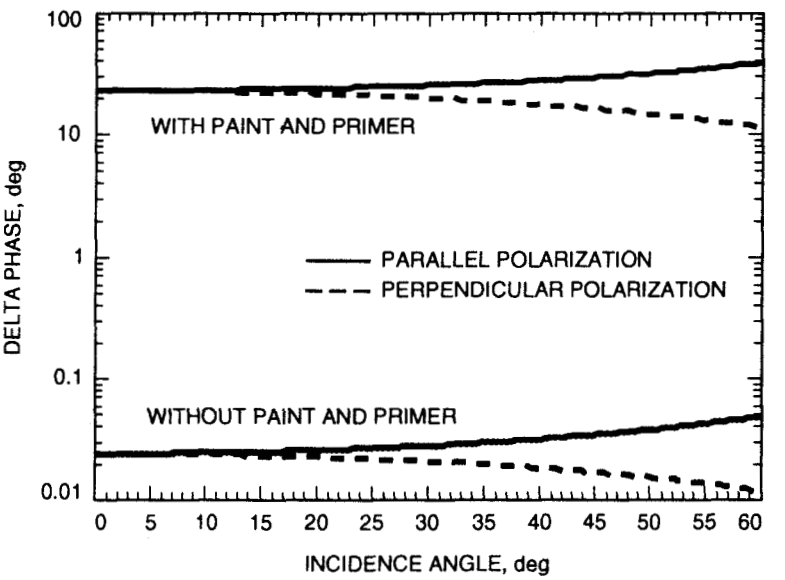

Figure 31. A comparison of delta phase with and without 0.254-mm (10-mil)-thick Triangle no. 6 paint and 0.0152-mm (0.6-mil)-thick zinc chromate primer on a flat 6061-T6 aluminum mirror.

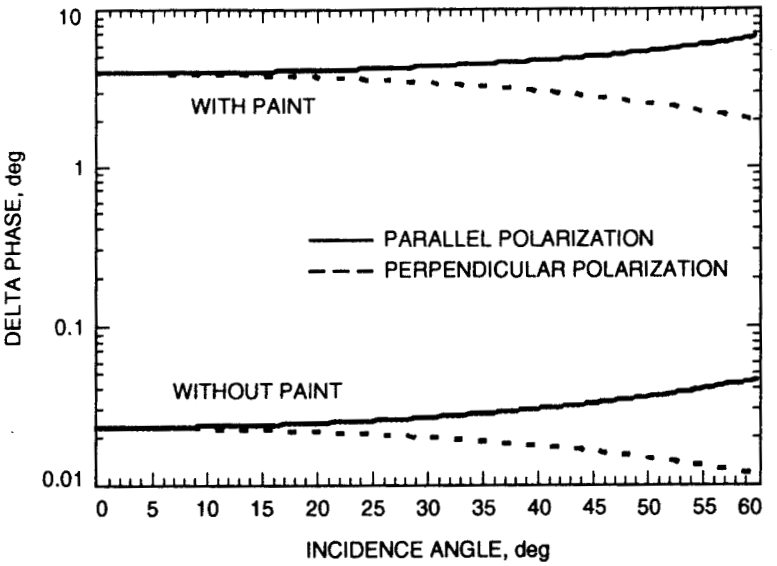

Figure 32. A comparison of delta phase with and without 0.0508-mm (2-mil)-thick 500FHR6 acrylic urethane-based paint on a flat 6061-T6 aluminum mirror.

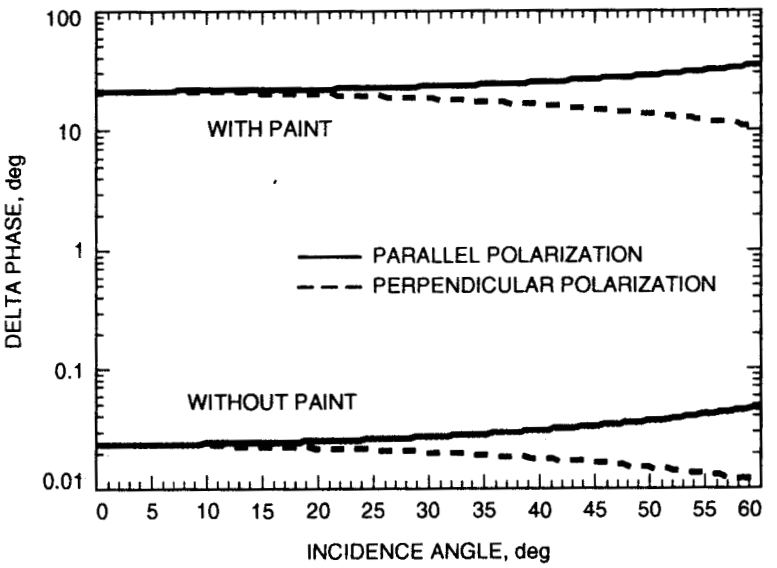

Figure 33. A comparison of delta phase with and without 0.254-mm (10-mil)-thick 500FHR6 paint with no primer on a flat 6061-T6 aluminum mirror.

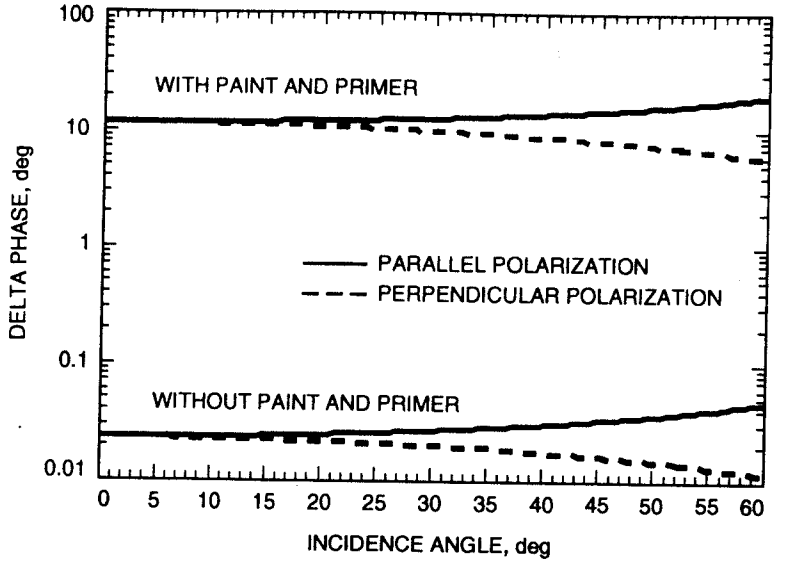

Figure 34. A comparison of delta phase with and without 0.127-mm (5-mil)-thick 18FHR6 water-based paint and 0.0152-mm (0.6-mil)-thick 283 water-based primer on a flat 6061-T6 aluminum mirror.

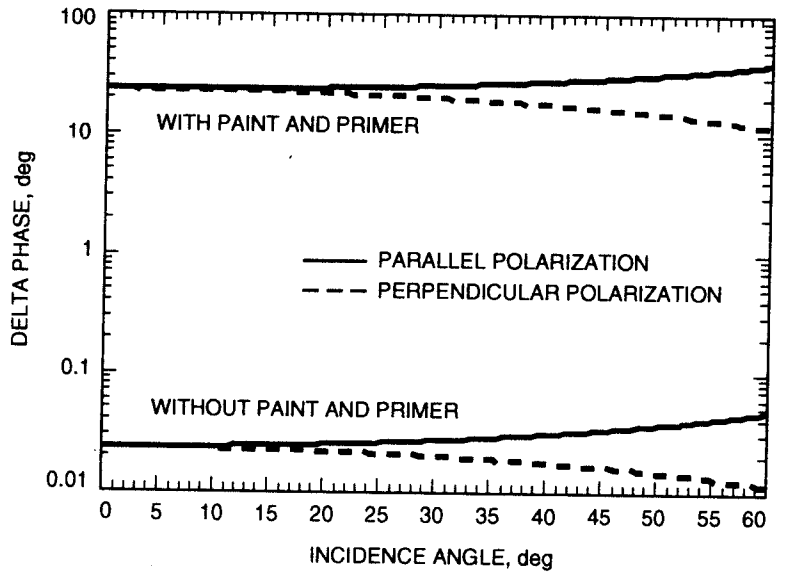

Figure 35. A comparison of delta phase with and without 0.254-mm (10-mil)-thick 18FHR6 water-based paint and 0.0152-mm (0.6-mil)-thick 283 water-based primer on a flat 6061-T6 aluminum mirror.

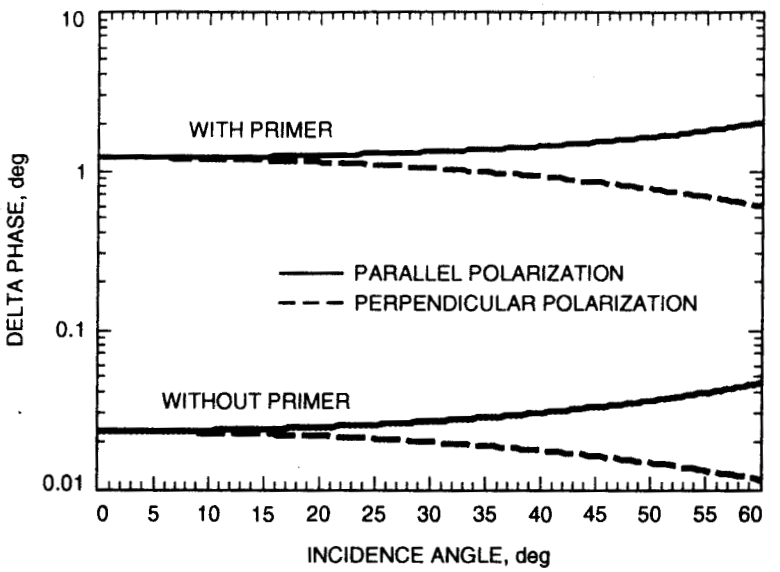

Figure 36. A comparison of delta phase with and without 0.0152-mm (0.6-mil)-thick zinc chromate primer on a flat 6061-T6 aluminum mirror.

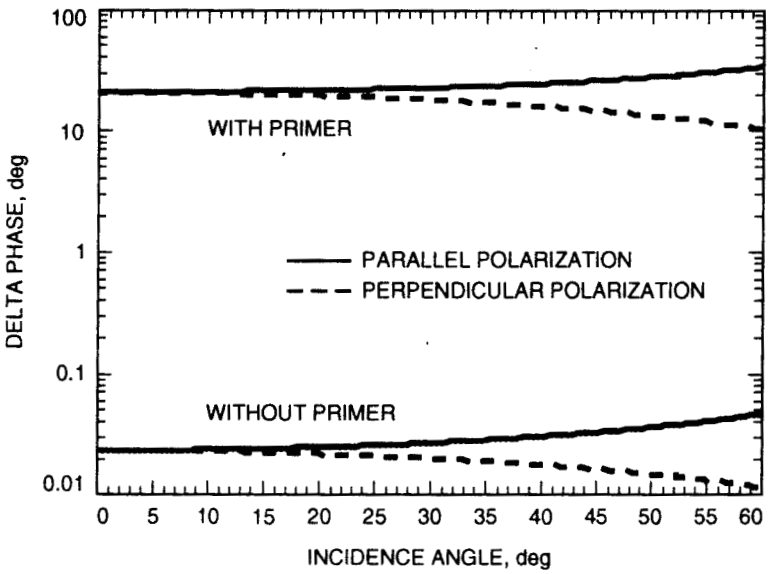

Figure 37. A comparison of delta phase with and without 0.254-mm (10-mil)-thick zinc chromate primer on a flat 6061-T6 aluminum mirror.